gprMax + MPI

Large-scale open-source computational electrodynamics

Antonis Giannopoulos • Nathan Mannall • Craig Warren and James Richings

THE UNIVERSITY of EDINBURGH

Northumbria University NEWCASTLE

epcc

What is gprMax?

"gprMax is a full-wave numerical modelling software package that is based on the finite-difference time-domain method for solving Maxwell's equations. It was initially developed to simulate the complex responses of ground penetrating radar systems. "

"gpr" from **"ground penetrating radar"** and **"Max"** from "Maxwell"

https://www.gprmax.com

https://github.com/gprmax/gprMax

http://docs.gprmax.com/en/latest/

What is GPR?

" … a term that describes both a piece of equipment - an Ultra Wide Band Radar - and a method to investigate into opaque objects and gather useful information about their composition.."

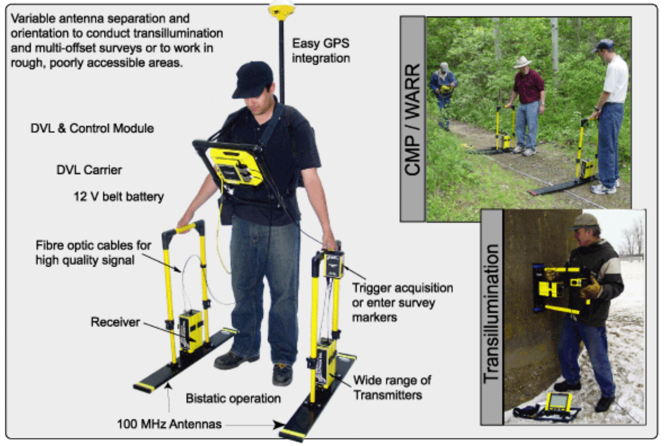

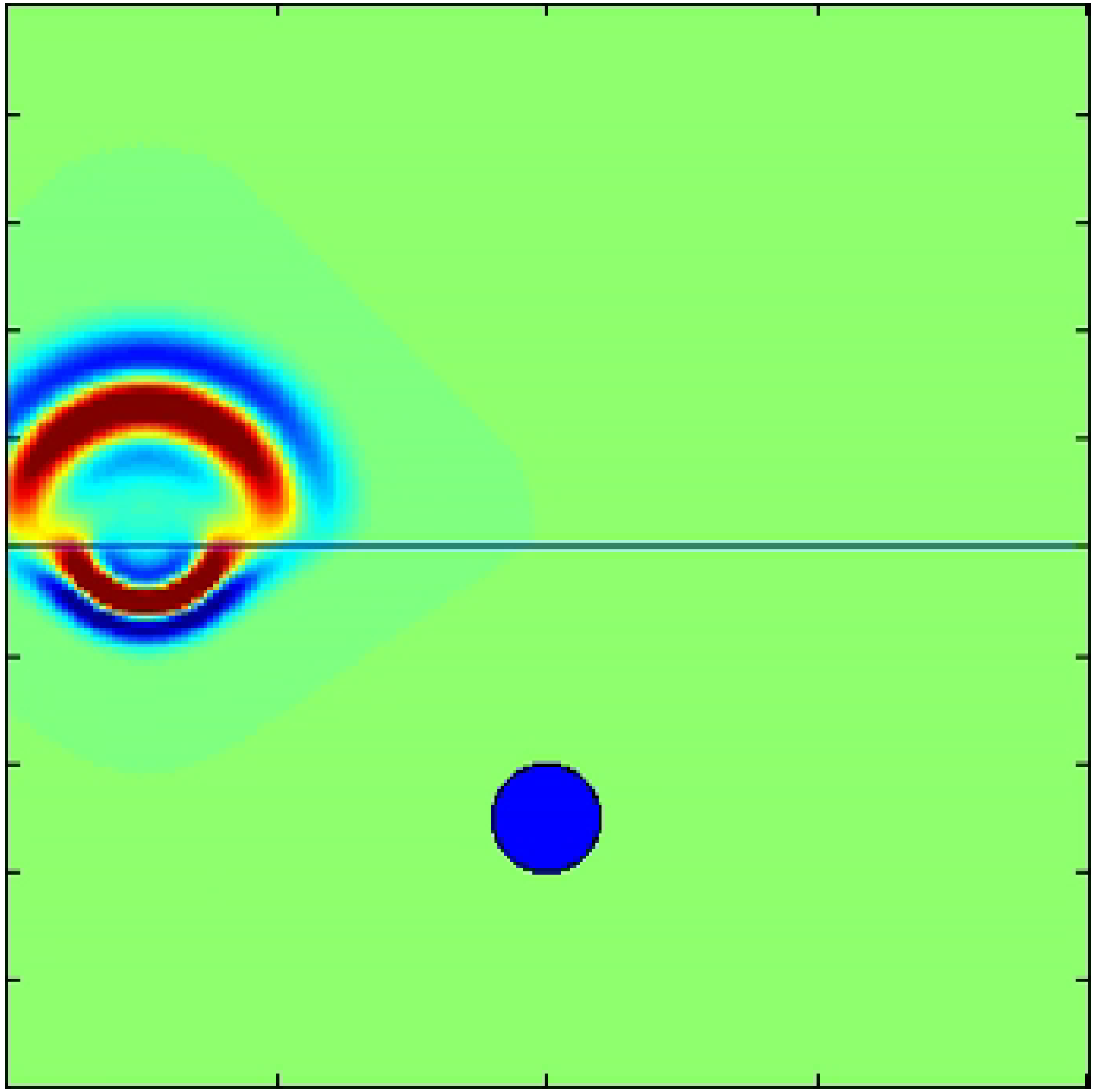

Heading

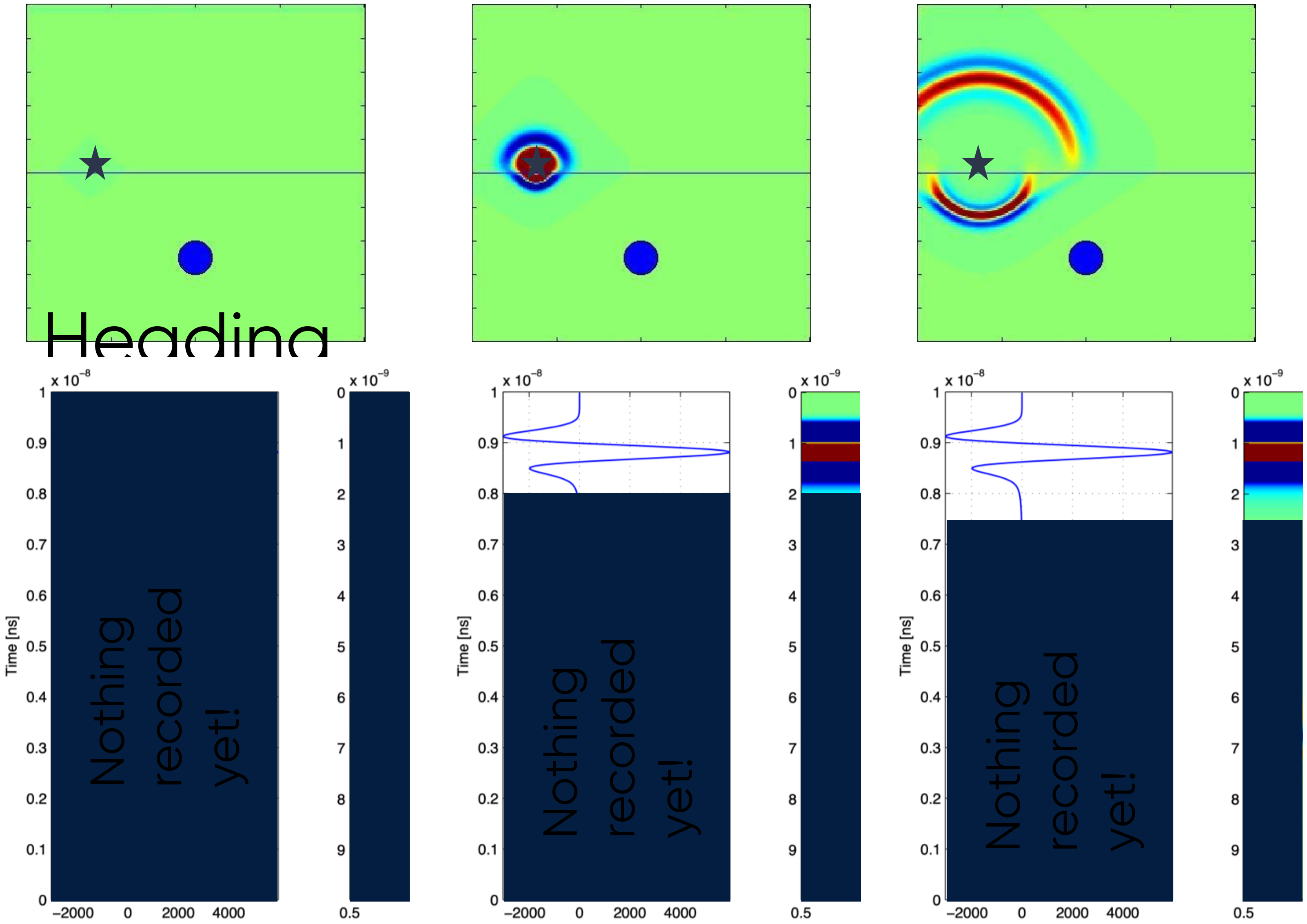
Nothing recorded yet!
Nothing recorded yet!
Nothing recorded yet!
Time [ns]
x 10^-8
x 10^-9
−2000
0
2000
4000
0.5

Heading

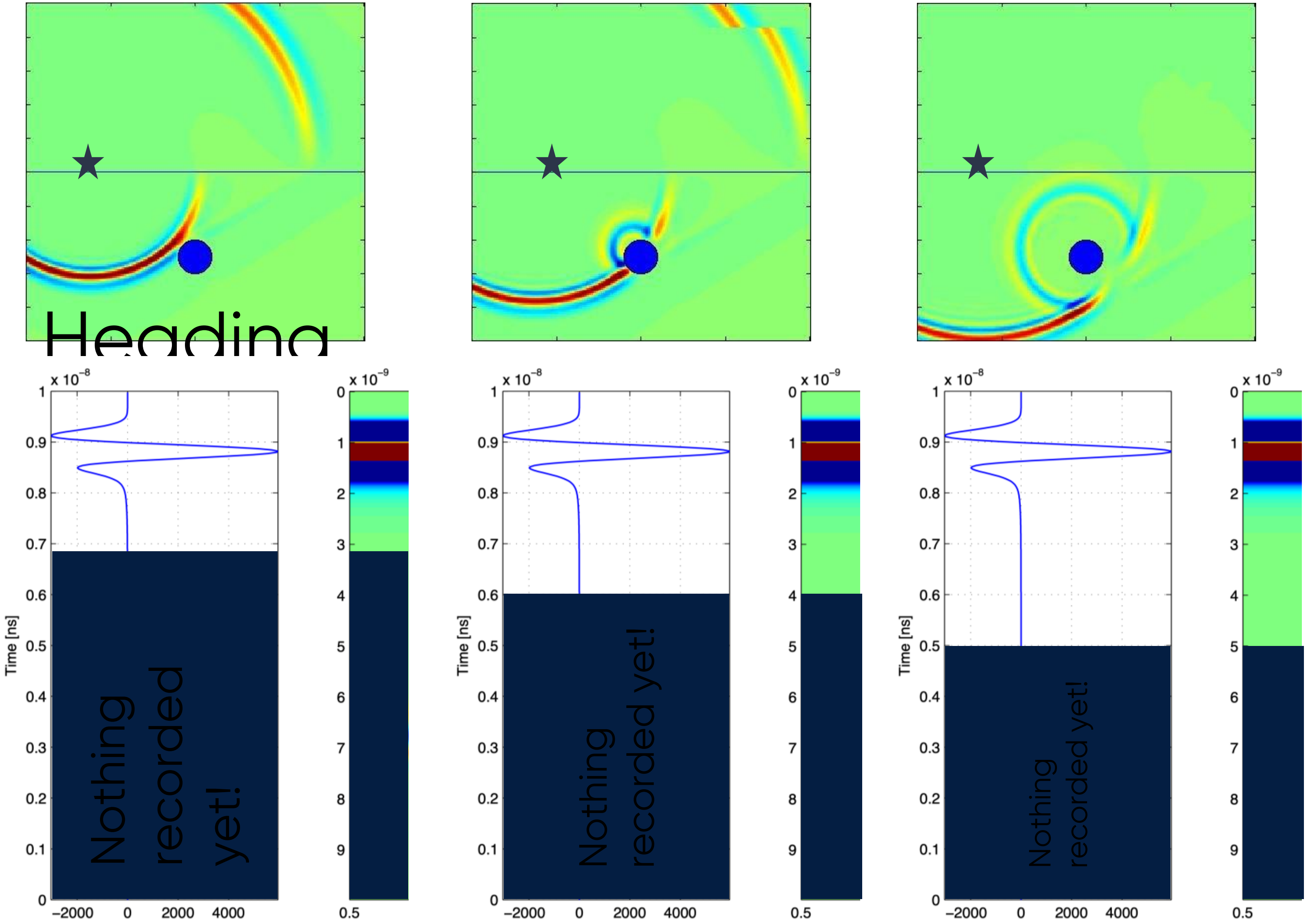

x 10^-8
x 10^-9
Time [ns]
Nothing recorded yet!
Nothing recorded yet!
Nothing recorded yet!

Heading

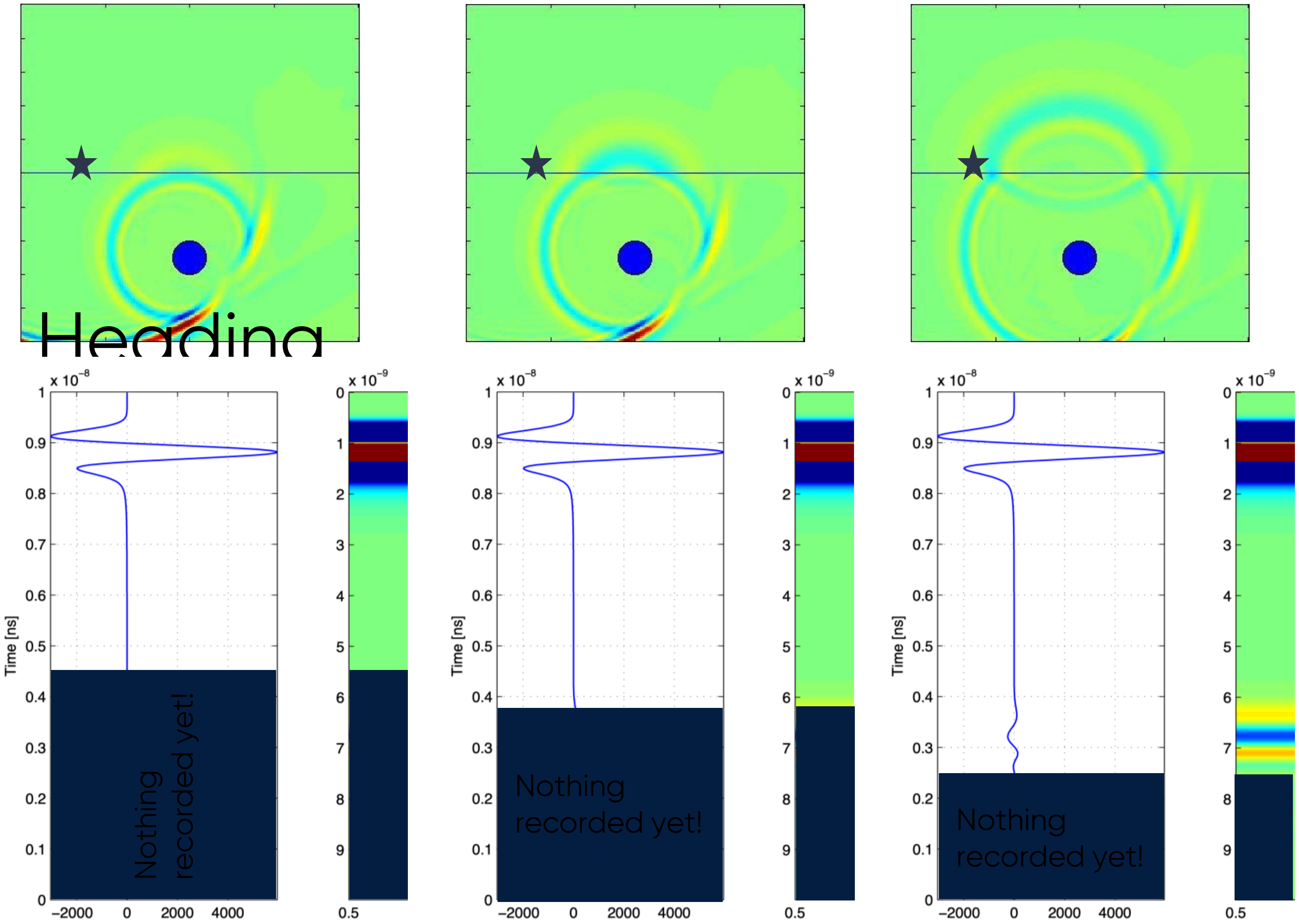

x 10^-8
x 10^-9
Time [ns]
Nothing recorded yet!
Nothing recorded yet!
Nothing recorded yet!

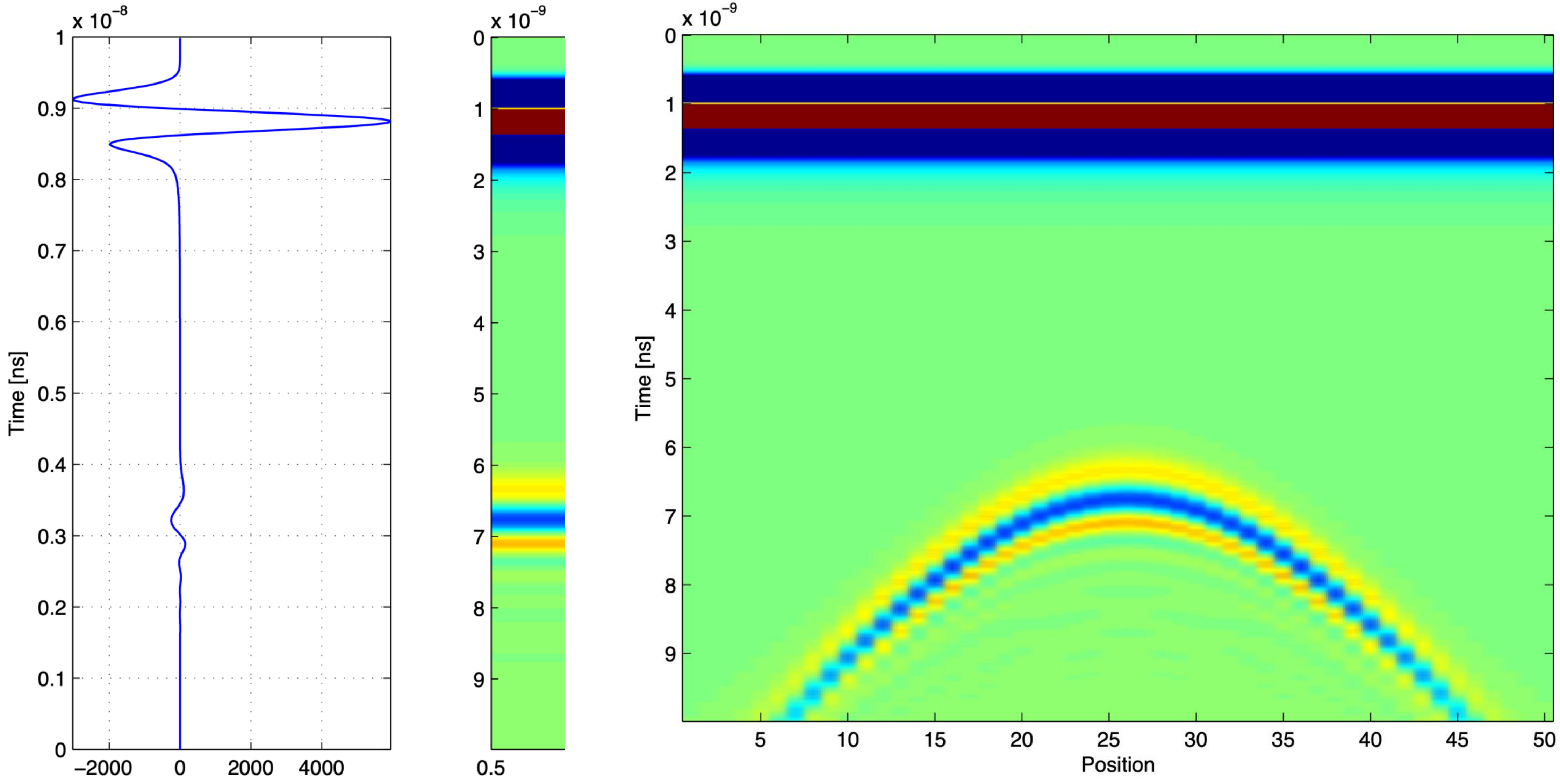
x 10^-8
Time [ns]
1
0.9
0.8
0.7
0.6
0.5
0.4
0.3
0.2
0.1
0
−2000
0
2000
4000
x 10^-9
0
1
2
3
4
5
6
7
8
9
0.5
x 10^-9
Time [ns]
0
1
2
3
4
5
6
7
8
9
5
10
15
20
25
30
35
40
45
50
Position

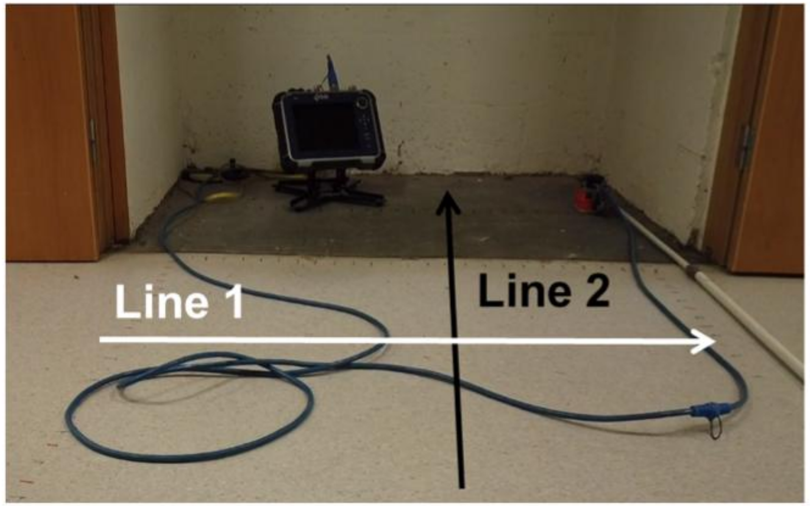
Line 1
Line 2

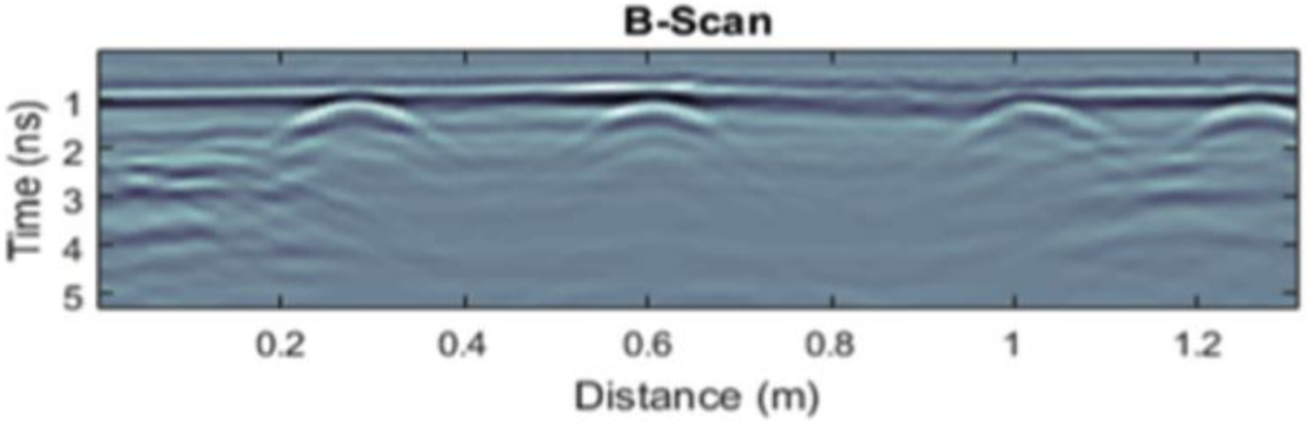
B-Scan
Time (ns)
1
2
3
4
5
0.2
0.4
0.6
0.8
1
1.2
Distance (m)

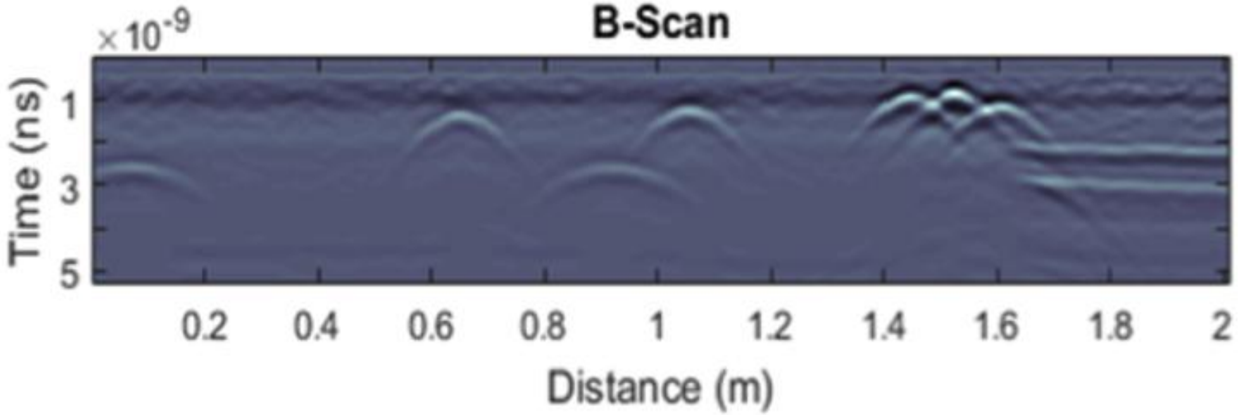
B-Scan
×10^-9
Time (ns)
1
3
5
0.2
0.4
0.6
0.8
1
1.2
1.4
1.6
1.8
2
Distance (m)

$$\oint_C \mathbf{E} \cdot d\hat{\mathbf{l}} = -\iint_S \frac{\partial \mathbf{B}}{\partial t} \cdot d\hat{\mathbf{s}}$$

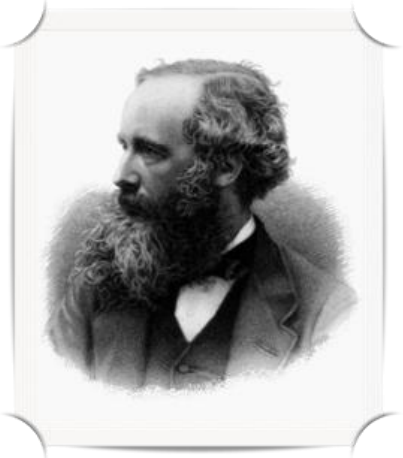

$$\oint_C \mathbf{H} \cdot d\hat{\mathbf{l}} = \iint_S \frac{\partial \mathbf{D}}{\partial t} \cdot d\hat{\mathbf{s}} + \iint_S \mathbf{J_c} \cdot d\hat{\mathbf{s}} + \iint_S \mathbf{J_s} \cdot d\hat{\mathbf{s}}$$

$$\oiint_S \mathbf{D} \cdot d\hat{\mathbf{s}} = \iiint_V q\,dV$$

$$\oiint_S \mathbf{B} \cdot d\hat{\mathbf{s}} = 0$$

The FDTD Yee cell

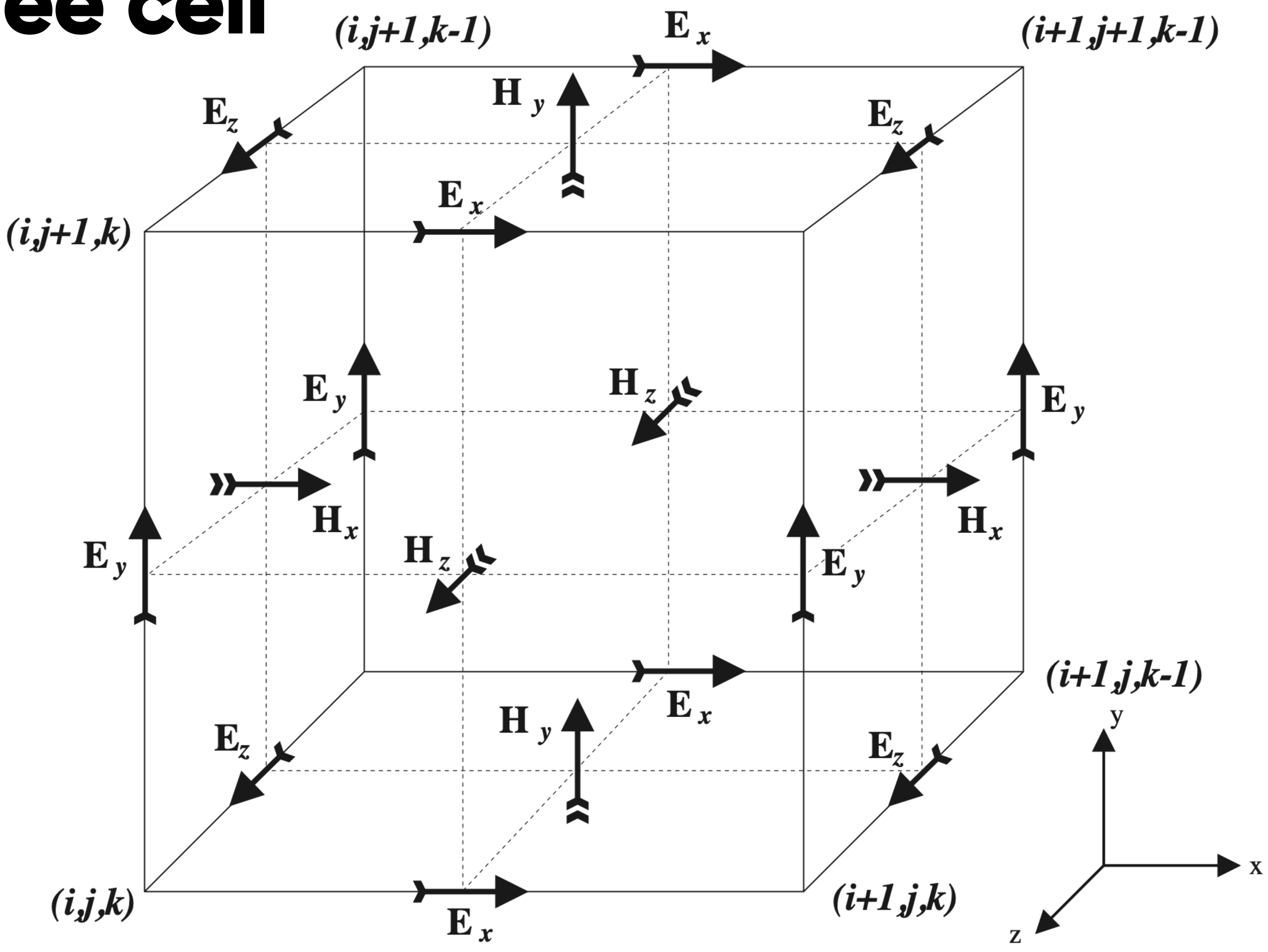

epcc

$$\oint_C \mathbf{H} \cdot d\hat{\mathbf{l}} = \iint_S \frac{\partial \mathbf{D}}{\partial t} \cdot d\hat{\mathbf{s}} + \iint_S \mathbf{J_c} \cdot d\hat{\mathbf{s}}$$

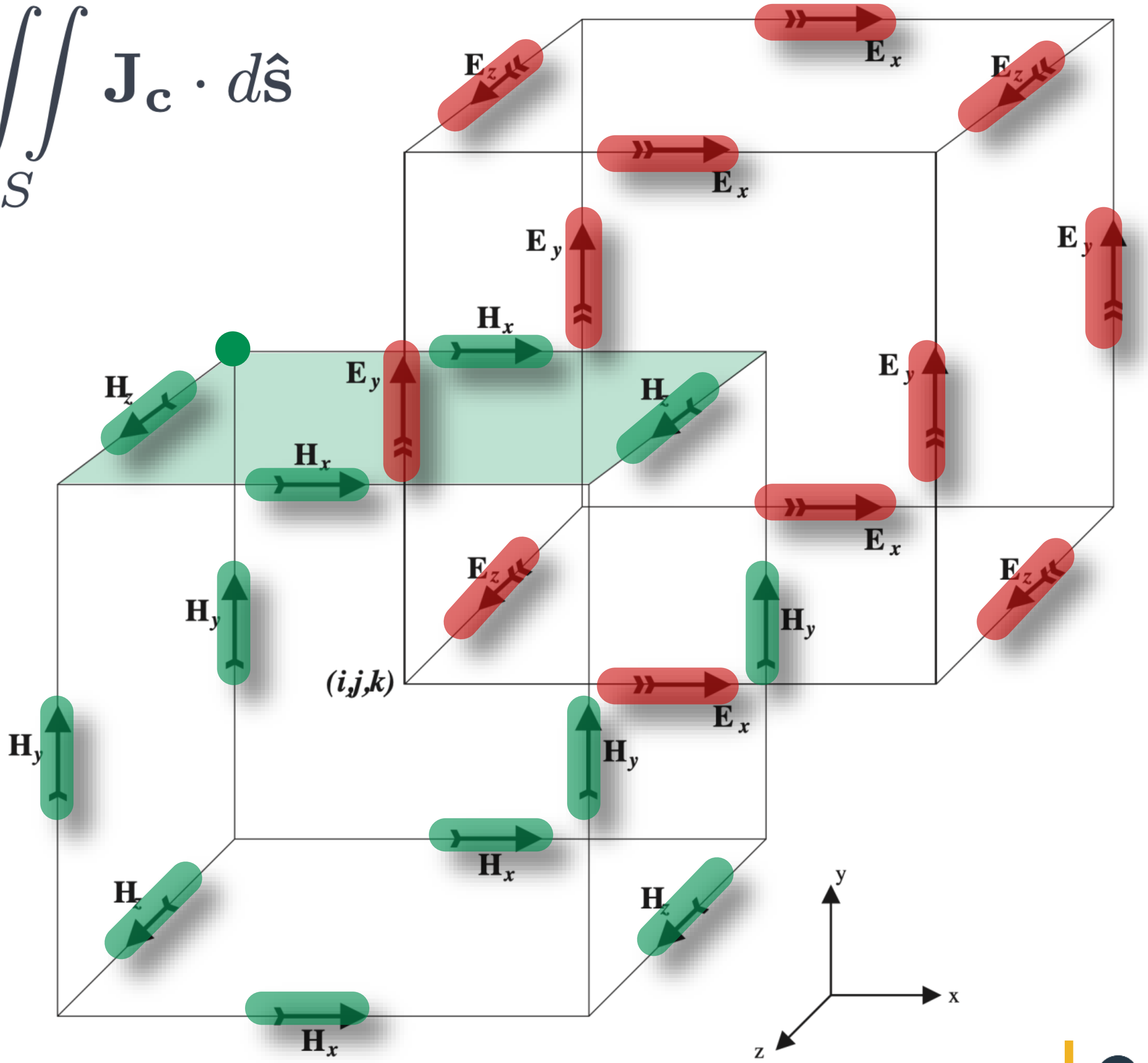

A short history of gprMax

1997

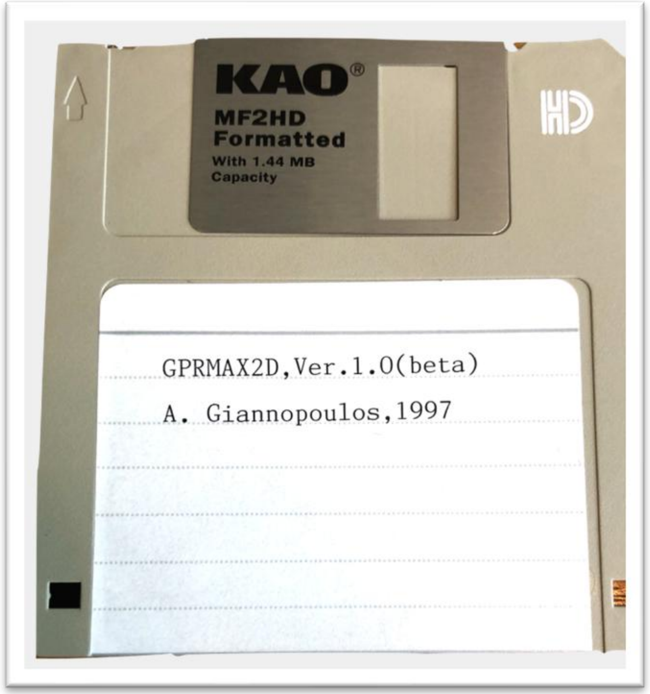
KAO
MF2HD
Formatted
With 1.44 MB
Capacity
GPRMAX2D,Ver.1.0(beta)
A. Giannopoulos,1997

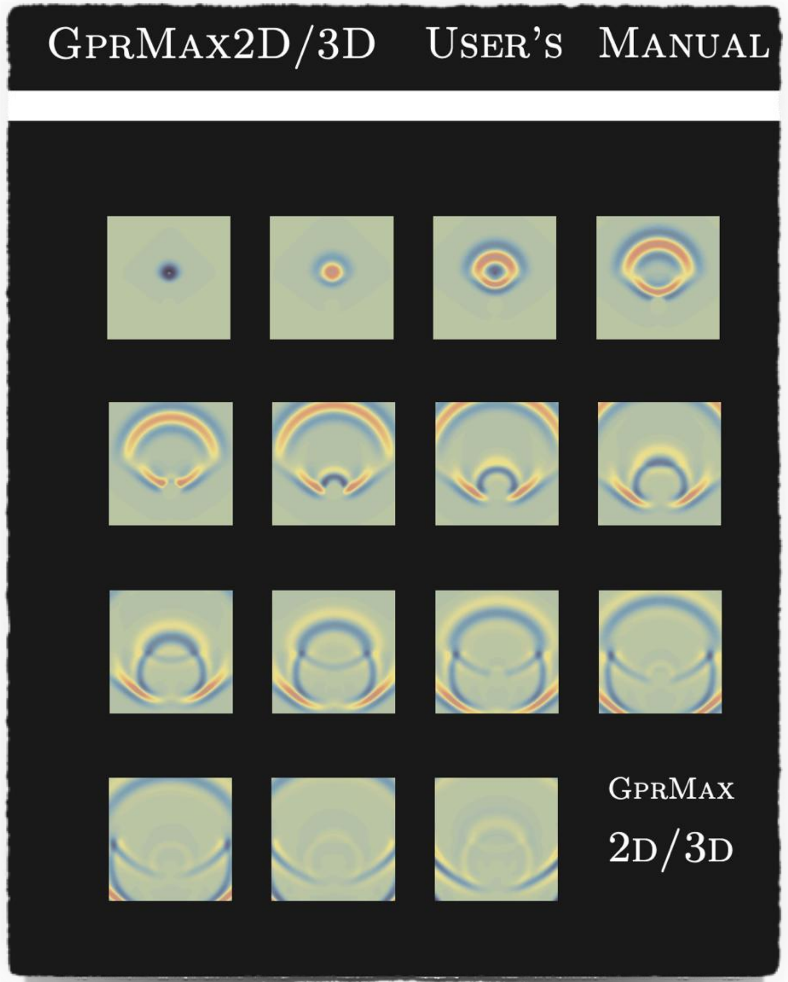
GprMax2D/3D User's Manual
GprMax
2D/3D

2015

gprMax
latest
Search docs

INTRODUCTION
Getting Started
Software Features
Guidance on GPR modelling

USING GPRMAX
Input file commands
Output data

PYTHON TOOLS
Plotting
File utilities

ADVANCED TOPICS
Scripting the input file
OpenMP, MPI, and HPC
GPGPU

USER LIBRARIES
GPR antenna models
Antenna patterns
AustinMan/AustinWoman
Materials
Optimisation - Taguchi's method

Docs » gprMax User Guide — Edit on GitHub

gprMax User Guide

Introduction

- Getting Started
  - What is gprMax?
  - Package overview
  - Installation
  - Running gprMax
  - Updating gprMax
- Software Features
  - What's new/changed?
  - Key features
- Guidance on GPR modelling
  - Basic concepts
  - Coordinate system and conventions
  - Spatial discretization
  - Absorbing boundary conditions

Using gprMax

- Input file commands
  - Essential commands
  - General commands
  - Material commands
  - Object construction commands
  - Source and output commands
  - PML commands

HTML
5
ePUB
PDF

GitHub

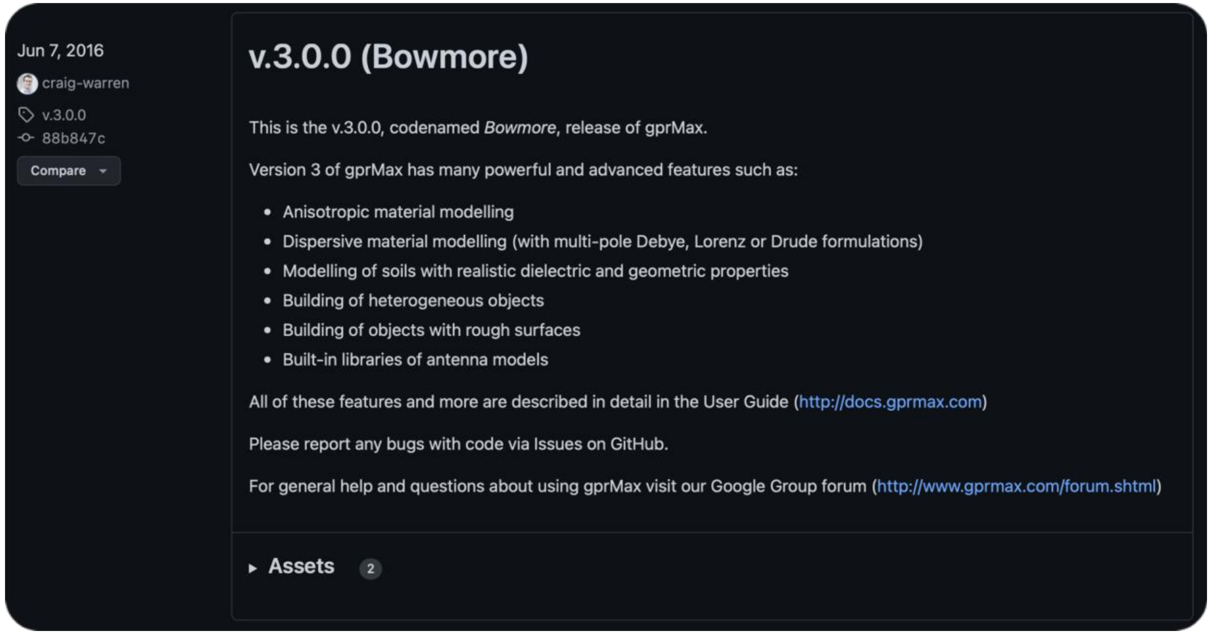

Jun 7, 2016
craig-warren
v.3.0.0
88b847c
Compare

v.3.0.0 (Bowmore)

This is the v.3.0.0, codenamed *Bowmore*, release of gprMax.

Version 3 of gprMax has many powerful and advanced features such as:

- Anisotropic material modelling
- Dispersive material modelling (with multi-pole Debye, Lorenz or Drude formulations)
- Modelling of soils with realistic dielectric and geometric properties
- Building of heterogeneous objects
- Building of objects with rough surfaces
- Built-in libraries of antenna models

All of these features and more are described in detail in the User Guide (http://docs.gprmax.com)

Please report any bugs with code via Issues on GitHub.

For general help and questions about using gprMax visit our Google Group forum (http://www.gprmax.com/forum.shtml)

Assets 2

python
Cython
C
The HDF Group
VTK
ParaView

epcc

Computer Physics Communications 209 (2016) 163–170

Contents lists available at ScienceDirect

Computer Physics Communications

journal homepage: www.elsevier.com/locate/cpc

gprMax: Open source software to simulate electromagnetic wave propagation for Ground Penetrating Radar☆

Craig Warren *, Antonios Giannopoulos, Iraklis Giannakis

Institute for Infrastructure and Environment, School of Engineering, The University of Edinburgh, Edinburgh, Scotland, United Kingdom

ARTICLE INFO

Article history:
Received 10 December 2015
Received in revised form
13 July 2016
Accepted 19 August 2016
Available online 8 September 2016

Keywords:
Computational electromagnetism
Ground Penetrating Radar
Finite-Difference Time-Domain
Open source
Python

ABSTRACT

gprMax is open source software that simulates electromagnetic wave propagation, using the Finite-Difference Time-Domain (FDTD) method, for the numerical modelling of Ground Penetrating Radar (GPR). gprMax was originally developed in 1996 when numerical modelling using the FDTD method and, in general, the numerical modelling of GPR were in their infancy. Current computing resources offer the opportunity to build detailed and complex FDTD models of GPR to an extent that was not previously possible. To enable these types of simulations to be more easily realised, and also to facilitate the addition of more advanced features, gprMax has been redeveloped and significantly modernised. The original C-based code has been completely rewritten using a combination of Python and Cython programming languages. Standard and robust file formats have been chosen for geometry and field output files. New advanced modelling features have been added including: an unsplit implementation of higher order Perfectly Matched Layers (PMLs) using a recursive integration approach; diagonally anisotropic materials; dispersive media using multi-pole Debye, Drude or Lorenz expressions; soil modelling using a semi-empirical formulation for dielectric properties and fractals for geometric characteristics; rough surface generation; and the ability to embed complex transducers and targets.

open source initiative

creative commons

GPL v3 Free Software

Free as in Freedom

epcc

2017

Jun 19, 2017
craig-warren
v.3.1.0
3c8e5ba
Compare

v.3.1.0 (Big Smoke)

This is the v.3.1.0, codenamed **Big Smoke**, release of gprMax.

It continues our whisky-based naming, and is also a reference to the cities of Edinburgh (Scotland) and San Francisco (USA). Why? Because the development of v.3.1.0 was funded, through a research project, by Google.

The most significant feature of this release is the ability for simulations to utilise **general-purpose computing using graphics processing units (GPGPU)**. We have used **NVIDIA's Compute-Unified Device Architecture (CUDA)**. Our testing on both consumer and data centre NVIDIA GPU cards has shown dramatic performance increases over our parallelised CPU (OpenMP) implementation.

You can read about how to use the GPU functionality and find all the features of gprMax described in detail in the User Guide (http://docs.gprmax.com)

Please report any bugs with code via Issues on GitHub.

For general help and questions about using gprMax visit our Google Group forum (http://www.gprmax.com/forum.shtml)

▸ Assets 2

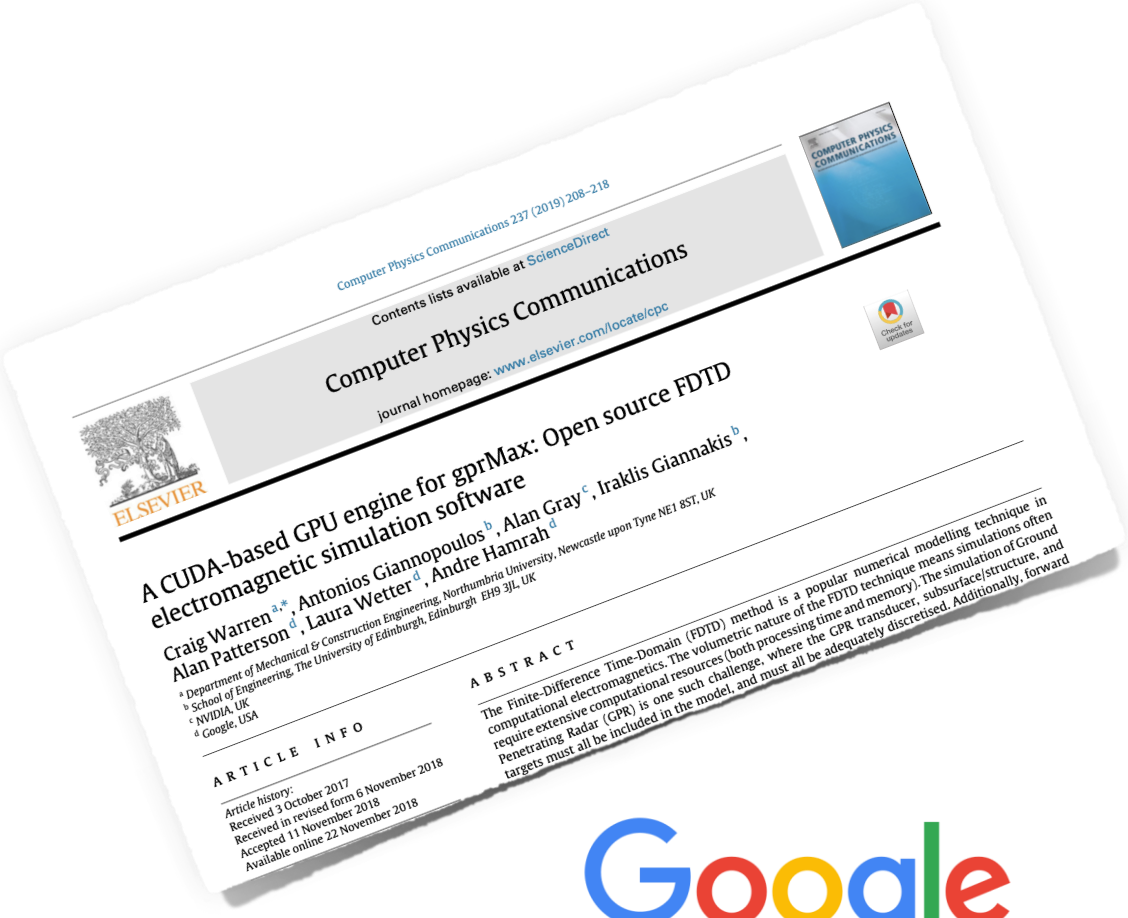
Computer Physics Communications 237 (2019) 208–218
Contents lists available at ScienceDirect
Computer Physics Communications
journal homepage: www.elsevier.com/locate/cpc

A CUDA-based GPU engine for gprMax: Open source FDTD electromagnetic simulation software

Craig Warren[a,*], Antonios Giannopoulos[b], Alan Gray[c], Iraklis Giannakis[b], Alan Patterson[d], Laura Wetter[d], Andre Hamrah[d]
[a] Department of Mechanical & Construction Engineering, Northumbria University, Newcastle upon Tyne NE1 8ST, UK
[b] School of Engineering, The University of Edinburgh, Edinburgh EH9 3JL, UK
[c] NVIDIA, UK
[d] Google, USA

A R T I C L E I N F O

Article history:
Received 3 October 2017
Received in revised form 6 November 2018
Accepted 11 November 2018
Available online 22 November 2018

A B S T R A C T

The Finite-Difference Time-Domain (FDTD) method is a popular numerical modelling technique in computational electromagnetics. The volumetric nature of the FDTD technique means simulations often require extensive computational resources (both processing time and memory). The simulation of Ground Penetrating Radar (GPR) is one such challenge, where the GPR transducer, subsurface/structure, and targets must all be included in the model, and must all be adequately discretised. Additionally, forward

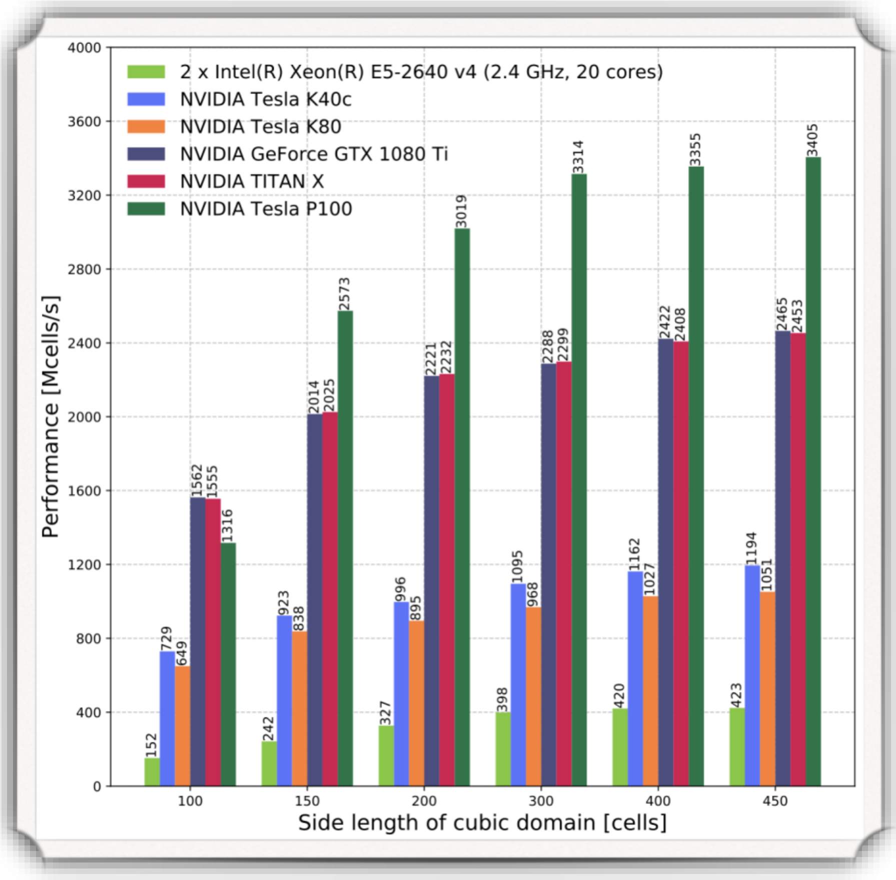

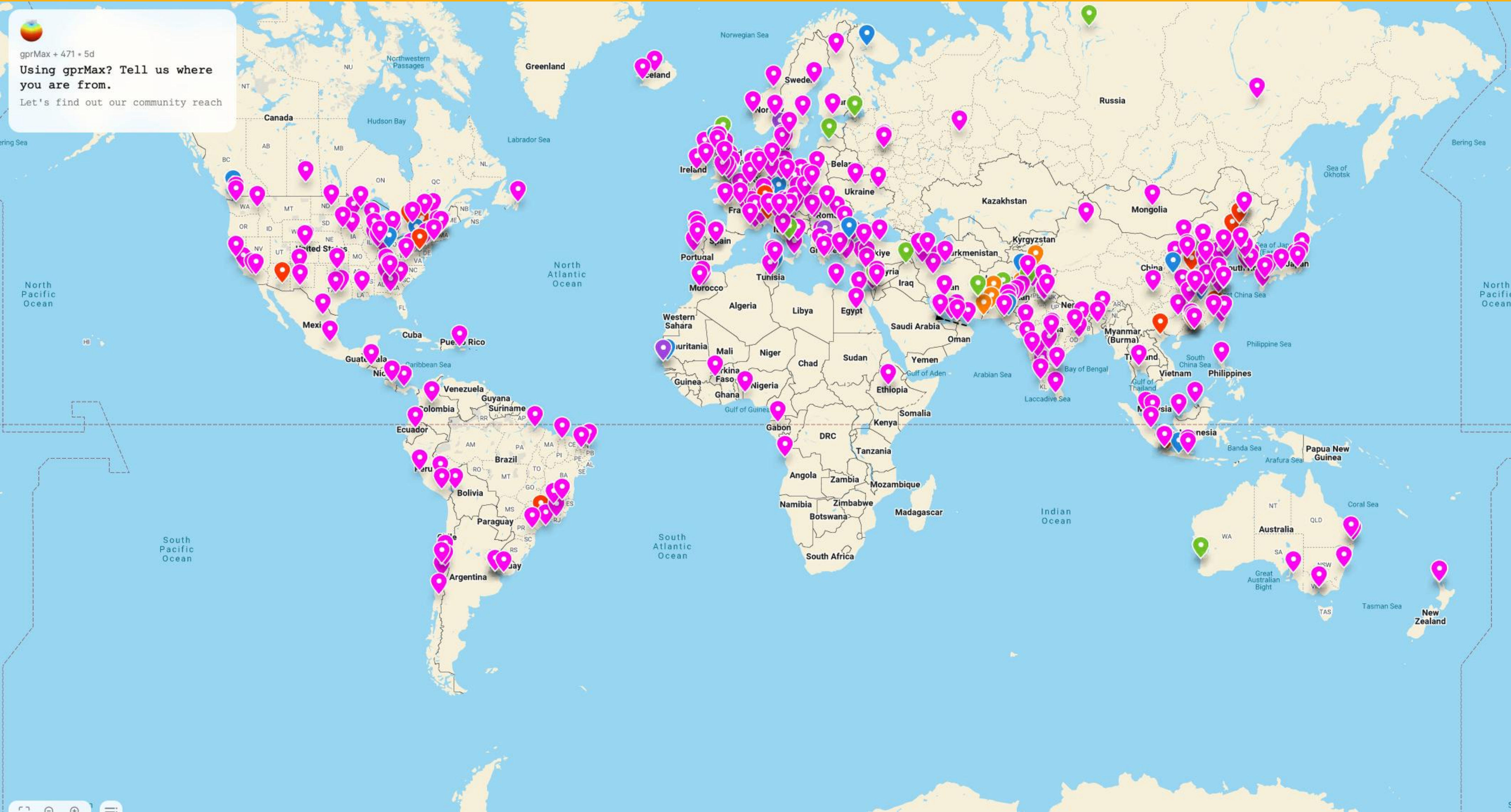

gprMax + 471 • 5d
Using gprMax? Tell us where you are from.
Let's find out our community reach
Greenland
Canada
Hudson Bay
Labrador Sea
Norwegian Sea
Russia
Kazakhstan
Mongolia
China
Japan
Ukraine
Ireland
Portugal
Morocco
Algeria
Libya
Egypt
Tunisia
Saudi Arabia
Iraq
Oman
Yemen
Western Sahara
Mali
Niger
Chad
Sudan
Ethiopia
Somalia
Kenya
Nigeria
Ghana
Guinea
Gabon
DRC
Tanzania
Angola
Zambia
Mozambique
Madagascar
Namibia
Zimbabwe
Botswana
South Africa
Vietnam
Philippines
Papua New Guinea
Australia
New Zealand
Cuba
Venezuela
Guyana
Suriname
Colombia
Ecuador
Brazil
Bolivia
Paraguay
Argentina
North Pacific Ocean
North Atlantic Ocean
South Pacific Ocean
South Atlantic Ocean
Indian Ocean
Arabian Sea
Bay of Bengal
Philippine Sea
Coral Sea
Tasman Sea
Bering Sea
Sea of Okhotsk
Caribbean Sea
Gulf of Guinea
Gulf of Aden
Banda Sea
Arafura Sea
Laccadive Sea

Publications

Cite gprMax

If you use gprMax and publish your work we would be grateful if you could cite our work!

The principal reference for gprMax is [1] which describes the new version of the software and its main features. If you have used specific elements of the software you might also like to cite: [2] - GPU accelerated solver, [3] - soil modelling, rough surfaces; [4] - dispersive materials; [5] - advanced features of the RIPML; [6, 7] - GPR antenna models. If you wish to reference the development history of gprMax you can also cite [8].

1. **Warren, C., Giannopoulos, A., & Giannakis, I. (2016). gprMax: Open source software to simulate electromagnetic wave propagation for Ground Penetrating Radar, *Computer Physics Communications*, *209*, 163-170,** 10.1016/j.cpc.2016.08.020.
2. Warren, C., Giannopoulos, A., Gray, A., Giannakis, I., Patterson, A., Wetter, L., & Hamrah, A. (2018). A CUDA-based GPU engine for gprMax: Open source FDTD electromagnetic simulation software, *Computer Physics Communications*, *237*, 208-218, 10.1016/j.cpc.2018.11.007.
3. Giannakis, I., Giannopoulos, A., Warren, C. (2016). A Realistic FDTD Numerical Modeling Framework of Ground Penetrating Radar for Landmine Detection. *IEEE Journal of Selected Topics in Applied Earth Observations and Remote Sensing*, *9*(1), 37-51, 10.1109/JSTARS.2015.2468597.
4. Giannakis, I., Giannopoulos, A. (2014). A Novel Piecewise Linear Recursive Convolution Approach for Dispersive Media Using the Finite-Difference Time-Domain Method. *IEEE Transactions on Antennas and Propagation*, *62*(5), 2669-2678, 10.1109/TAP.2014.2308549.
5. Giannopoulos, A. (2012). Unsplit Implementation of Higher Order PMLs. *IEEE Transactions on Antennas and Propagation*, *60*(3), 1479-1485, 10.1109/TAP.2011.2180344.
6. Warren, C., Giannopoulos, A. (2011). Creating finite-difference time-domain models of commercial ground-penetrating radar antennas using Taguchi's optimization method. *Geophysics*, *76*(2), G37-G47, 10.1190/1.3548506.
7. Giannakis, I., Giannopoulos, A., Warren, C. (2018). Realistic FDTD GPR antenna models optimised using a novel linear/non-linear Full Waveform Inversion. *IEEE Transactions on Geoscience & Remote Sensing*, *207*(3), 1768-1778, 10.1109/TGRS.2018.2869027.
8. Giannopoulos, A. (2005). Modelling ground penetrating radar by GprMax, *Construction and Building Materials*, *19*(10), 755-762, 10.1016/j.conbuildmat.2005.06.007.

You can also get references and links to the PhD theses of the development team.

Research using gprMax

gprMax has been successfully used for a diverse range of applications in academia and industry, from fields including **engineering**, **geophysics**, **archaeology**, and **medicine**. The following table lists publications (extracted from Scopus on 23-11-2025) that have cited references [1], [2] and [8] excluding any self-citations of the authors.

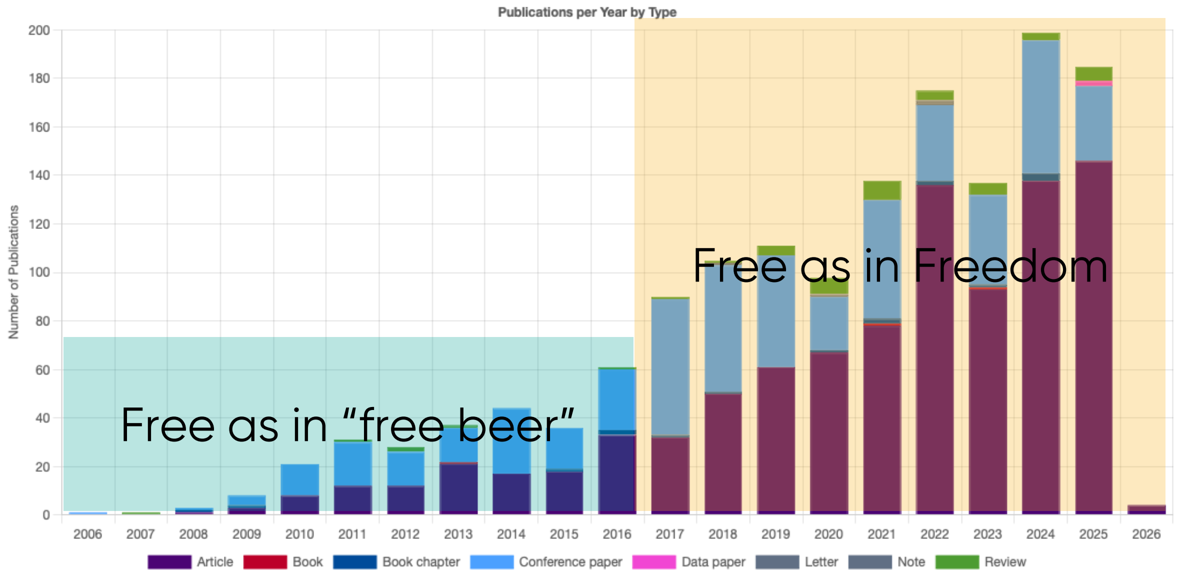

Basic capabilities

Our own Recursive integration perfectly matched layer (PML) implementation for higher order and multipole PMLs

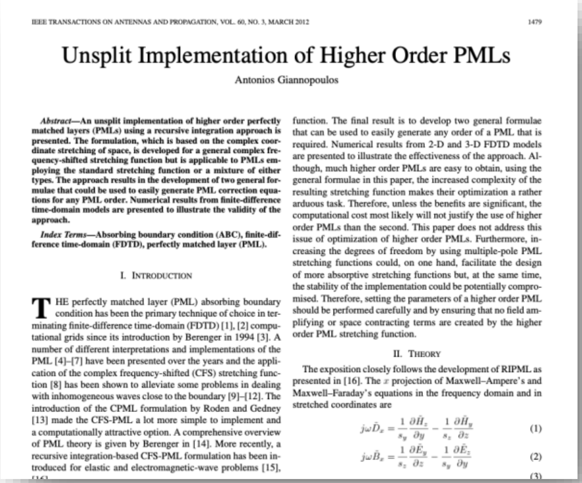

IEEE TRANSACTIONS ON ANTENNAS AND PROPAGATION, VOL. 60, NO. 3, MARCH 2012 1479

Unsplit Implementation of Higher Order PMLs

Antonios Giannopoulos

***Abstract*—An unsplit implementation of higher order perfectly matched layers (PMLs) using a recursive integration approach is presented. The formulation, which is based on the complex coordinate stretching of space, is developed for a general complex frequency-shifted stretching function but is applicable to PMLs employing the standard stretching function or a mixture of either types. The approach results in the development of two general formulae that could be used to easily generate PML correction equations for any PML order. Numerical results from finite-difference time-domain models are presented to illustrate the validity of the approach.**

***Index Terms*—Absorbing boundary condition (ABC), finite-difference time-domain (FDTD), perfectly matched layer (PML).**

I. Introduction

THE perfectly matched layer (PML) absorbing boundary condition has been the primary technique of choice in terminating finite-difference time-domain (FDTD) [1], [2] computational grids since its introduction by Berenger in 1994 [3]. A number of different interpretations and implementations of the PML [4]–[7] have been presented over the years and the application of the complex frequency-shifted (CFS) stretching function [8] has been shown to alleviate some problems in dealing with inhomogeneous waves close to the boundary [9]–[12]. The introduction of the CPML formulation by Roden and Gedney [13] made the CFS-PML a lot more simple to implement and a computationally attractive option. A comprehensive overview of PML theory is given by Berenger in [14]. More recently, a recursive integration-based CFS-PML formulation has been introduced for elastic and electromagnetic-wave problems [15], [16] ... function. The final result is to develop two general formulae that can be used to easily generate any order of a PML that is required. Numerical results from 2-D and 3-D FDTD models are presented to illustrate the effectiveness of the approach. Although, much higher order PMLs are easy to obtain, using the general formulae in this paper, the increased complexity of the resulting stretching function makes their optimization a rather arduous task. Therefore, unless the benefits are significant, the computational cost most likely will not justify the use of higher order PMLs than the second. This paper does not address this issue of optimization of higher order PMLs. Furthermore, increasing the degrees of freedom by using multiple-pole PML stretching functions could, on one hand, facilitate the design of more absorptive stretching functions but, at the same time, the stability of the implementation could be potentially compromised. Therefore, setting the parameters of a higher order PML should be performed carefully and by ensuring that no field amplifying or space contracting terms are created by the higher order PML stretching function.

II. Theory

The exposition closely follows the development of RIPML as presented in [16]. The x projection of Maxwell–Ampere's and Maxwell–Faraday's equations in the frequency domain and in stretched coordinates are

$$j\omega\tilde{D}_x = \frac{1}{s_y}\frac{\partial\tilde{H}_z}{\partial y} - \frac{1}{s_z}\frac{\partial\tilde{H}_y}{\partial z} \quad (1)$$

$$j\omega\tilde{B}_x = \frac{1}{s_z}\frac{\partial\tilde{E}_y}{\partial z} - \frac{1}{s_y}\frac{\partial\tilde{E}_z}{\partial y} \quad (2)$$

(3)

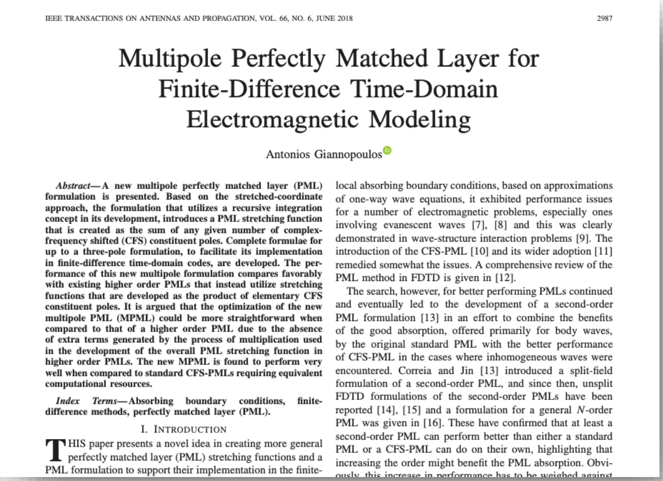

IEEE TRANSACTIONS ON ANTENNAS AND PROPAGATION, VOL. 66, NO. 6, JUNE 2018 2987

Multipole Perfectly Matched Layer for Finite-Difference Time-Domain Electromagnetic Modeling

Antonios Giannopoulos

***Abstract*—A new multipole perfectly matched layer (PML) formulation is presented. Based on the stretched-coordinate approach, the formulation that utilizes a recursive integration concept in its development, introduces a PML stretching function that is created as the sum of any given number of complex-frequency shifted (CFS) constituent poles. Complete formulae for up to a three-pole formulation, to facilitate its implementation in finite-difference time-domain codes, are developed. The performance of this new multipole formulation compares favorably with existing higher order PMLs that instead utilize stretching functions that are developed as the product of elementary CFS constituent poles. It is argued that the optimization of the new multipole PML (MPML) could be more straightforward when compared to that of a higher order PML due to the absence of extra terms generated by the process of multiplication used in the development of the overall PML stretching function in higher order PMLs. The new MPML is found to perform very well when compared to standard CFS-PMLs requiring equivalent computational resources.**

***Index Terms*—Absorbing boundary conditions, finite-difference methods, perfectly matched layer (PML).**

I. Introduction

THIS paper presents a novel idea in creating more general perfectly matched layer (PML) stretching functions and a PML formulation to support their implementation in the finite- ... local absorbing boundary conditions, based on approximations of one-way wave equations, it exhibited performance issues for a number of electromagnetic problems, especially ones involving evanescent waves [7], [8] and this was clearly demonstrated in wave-structure interaction problems [9]. The introduction of the CFS-PML [10] and its wider adoption [11] remedied somewhat the issues. A comprehensive review of the PML method in FDTD is given in [12].

The search, however, for better performing PMLs continued and eventually led to the development of a second-order PML formulation [13] in an effort to combine the benefits of the good absorption, offered primarily for body waves, by the original standard PML with the better performance of CFS-PML in the cases where inhomogeneous waves were encountered. Correia and Jin [13] introduced a split-field formulation of a second-order PML, and since then, unsplit FDTD formulations of the second-order PMLs have been reported [14], [15] and a formulation for a general N-order PML was given in [16]. These have confirmed that at least a second-order PML can perform better than either a standard PML or a CFS-PML can do on their own, highlighting that increasing the order might benefit the PML absorption. Obviously, this increase in performance has to be weighed against

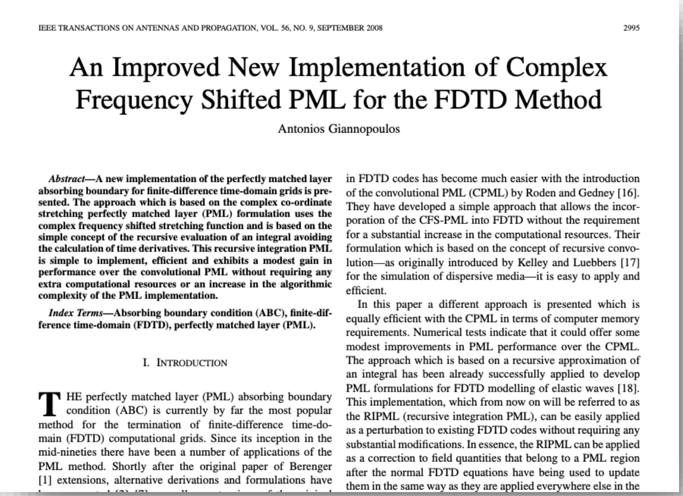

IEEE TRANSACTIONS ON ANTENNAS AND PROPAGATION, VOL. 56, NO. 9, SEPTEMBER 2008 2995

An Improved New Implementation of Complex Frequency Shifted PML for the FDTD Method

Antonios Giannopoulos

***Abstract*—A new implementation of the perfectly matched layer absorbing boundary for finite-difference time-domain grids is presented. The approach which is based on the complex co-ordinate stretching perfectly matched layer (PML) formulation uses the complex frequency shifted stretching function and is based on the simple concept of the recursive evaluation of an integral avoiding the calculation of time derivatives. This recursive integration PML is simple to implement, efficient and exhibits a modest gain in performance over the convolutional PML without requiring any extra computational resources or an increase in the algorithmic complexity of the PML implementation.**

***Index Terms*—Absorbing boundary condition (ABC), finite-difference time-domain (FDTD), perfectly matched layer (PML).**

I. Introduction

THE perfectly matched layer (PML) absorbing boundary condition (ABC) is currently by far the most popular method for the termination of finite-difference time-domain (FDTD) computational grids. Since its inception in the mid-nineties there have been a number of applications of the PML method. Shortly after the original paper of Berenger [1] extensions, alternative derivations and formulations have ... in FDTD codes has become much easier with the introduction of the convolutional PML (CPML) by Roden and Gedney [16]. They have developed a simple approach that allows the incorporation of the CFS-PML into FDTD without the requirement for a substantial increase in the computational resources. Their formulation which is based on the concept of recursive convolution—as originally introduced by Kelley and Luebbers [17] for the simulation of dispersive media—it is easy to apply and efficient.

In this paper a different approach is presented which is equally efficient with the CPML in terms of computer memory requirements. Numerical tests indicate that it could offer some modest improvements in PML performance over the CPML. The approach which is based on a recursive approximation of an integral has been already successfully applied to develop PML formulations for FDTD modelling of elastic waves [18]. This implementation, which from now on will be referred to as the RIPML (recursive integration PML), can be easily applied as a perturbation to existing FDTD codes without requiring any substantial modifications. In essence, the RIPML can be applied as a correction to field quantities that belong to a PML region after the normal FDTD equations have being used to update them in the same way as they are applied everywhere else in the

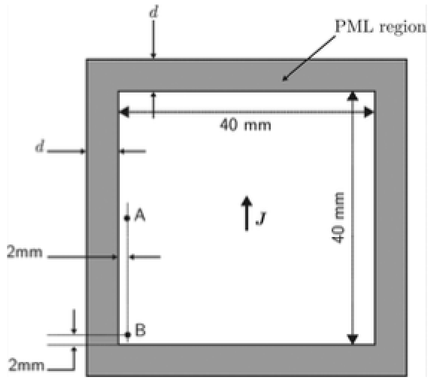

Fig. 1. Model of a y-directed electric current source at the centre of a 40 × 40 1 mm cell TE_z FDTD grid. The computational domain is surrounded by a PML of thickness d. The E_y fields are sampled at points A and B [20, Ch. 7].

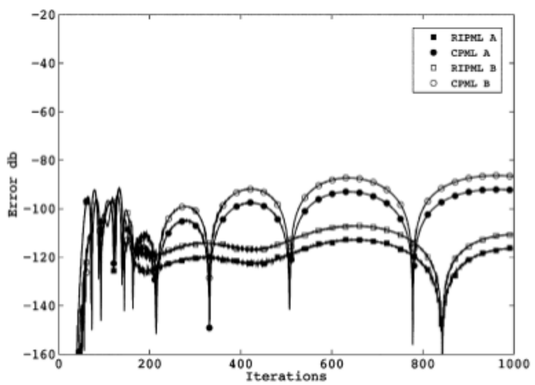

Fig. 3. Error in the E_y field component at points A and B for models terminated using RIPML and CPML. $\kappa_{\max} = 1$ and $\alpha_{\max} = 0.2$.

epcc

Our own very accurate dispersive media model

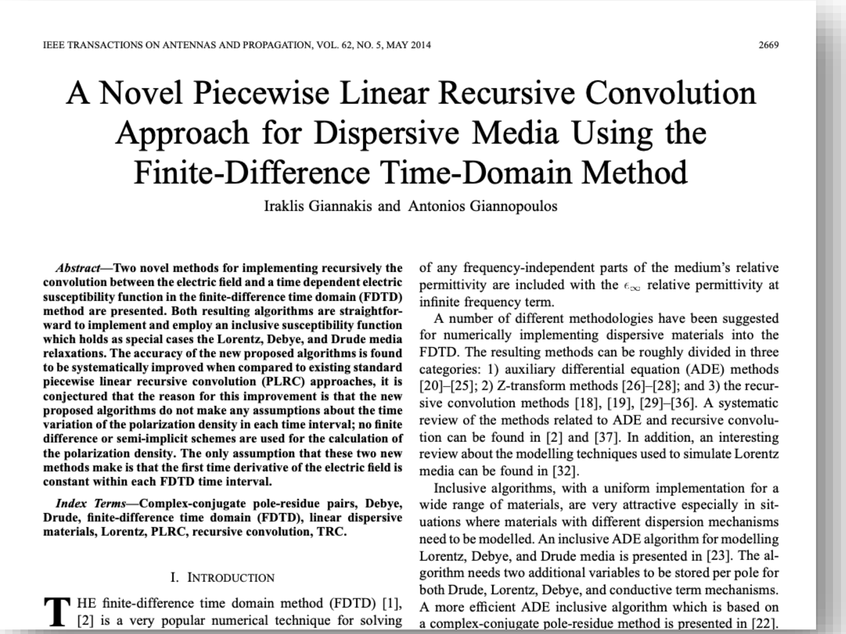

IEEE TRANSACTIONS ON ANTENNAS AND PROPAGATION, VOL. 62, NO. 5, MAY 2014 2669

A Novel Piecewise Linear Recursive Convolution Approach for Dispersive Media Using the Finite-Difference Time-Domain Method

Iraklis Giannakis and Antonios Giannopoulos

Abstract—Two novel methods for implementing recursively the convolution between the electric field and a time dependent electric susceptibility function in the finite-difference time domain (FDTD) method are presented. Both resulting algorithms are straightforward to implement and employ an inclusive susceptibility function which holds as special cases the Lorentz, Debye, and Drude media relaxations. The accuracy of the new proposed algorithms is found to be systematically improved when compared to existing standard piecewise linear recursive convolution (PLRC) approaches, it is conjectured that the reason for this improvement is that the new proposed algorithms do not make any assumptions about the time variation of the polarization density in each time interval; no finite difference or semi-implicit schemes are used for the calculation of the polarization density. The only assumption that these two new methods make is that the first time derivative of the electric field is constant within each FDTD time interval.

Index Terms—Complex-conjugate pole-residue pairs, Debye, Drude, finite-difference time domain (FDTD), linear dispersive materials, Lorentz, PLRC, recursive convolution, TRC.

I. Introduction

THE finite-difference time domain method (FDTD) [1], [2] is a very popular numerical technique for solving

of any frequency-independent parts of the medium's relative permittivity are included with the ϵ_∞ relative permittivity at infinite frequency term.

A number of different methodologies have been suggested for numerically implementing dispersive materials into the FDTD. The resulting methods can be roughly divided in three categories: 1) auxiliary differential equation (ADE) methods [20]–[25]; 2) Z-transform methods [26]–[28]; and 3) the recursive convolution methods [18], [19], [29]–[36]. A systematic review of the methods related to ADE and recursive convolution can be found in [2] and [37]. In addition, an interesting review about the modelling techniques used to simulate Lorentz media can be found in [32].

Inclusive algorithms, with a uniform implementation for a wide range of materials, are very attractive especially in situations where materials with different dispersion mechanisms need to be modelled. An inclusive ADE algorithm for modelling Lorentz, Debye, and Drude media is presented in [23]. The algorithm needs two additional variables to be stored per pole for both Drude, Lorentz, Debye, and conductive term mechanisms. A more efficient ADE inclusive algorithm which is based on a complex-conjugate pole-residue method is presented in [22].

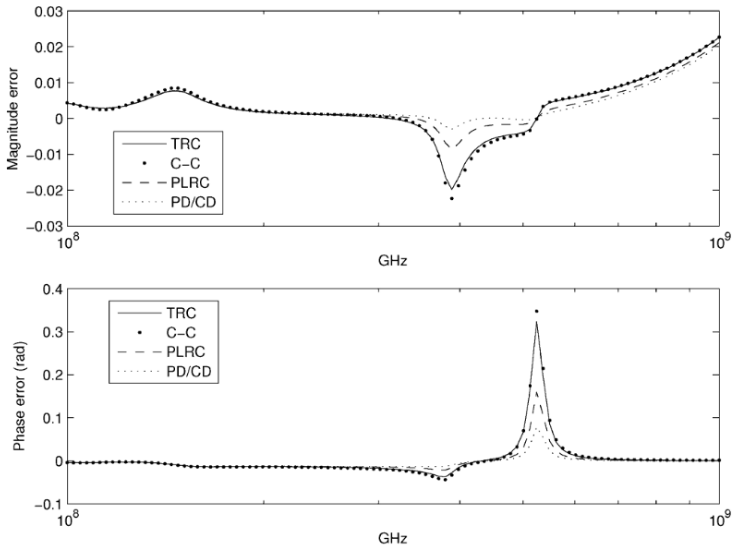

Fig. 4. Multi-Lorentz medium: Error between analytical and numerical reflection coefficients for TRC, PLRC, Complex-Conjugate (C-C) method, Current Density method (CD), and Polarization Density method (PD).

Multi Debye, Drude and Lorentz materials and functionality that allows you to fit using multiple Debye poles arbitrary complex permittivity data

Diagonally anisotropic materials

$$\bar{\bar{\epsilon}} = \begin{bmatrix} \epsilon_{xx} & 0 & 0 \\ 0 & \epsilon_{yy} & 0 \\ 0 & 0 & \epsilon_{zz} \end{bmatrix}$$

$$\bar{\bar{\sigma}} = \begin{bmatrix} \sigma_{xx} & 0 & 0 \\ 0 & \sigma_{yy} & 0 \\ 0 & 0 & \sigma_{zz} \end{bmatrix}$$

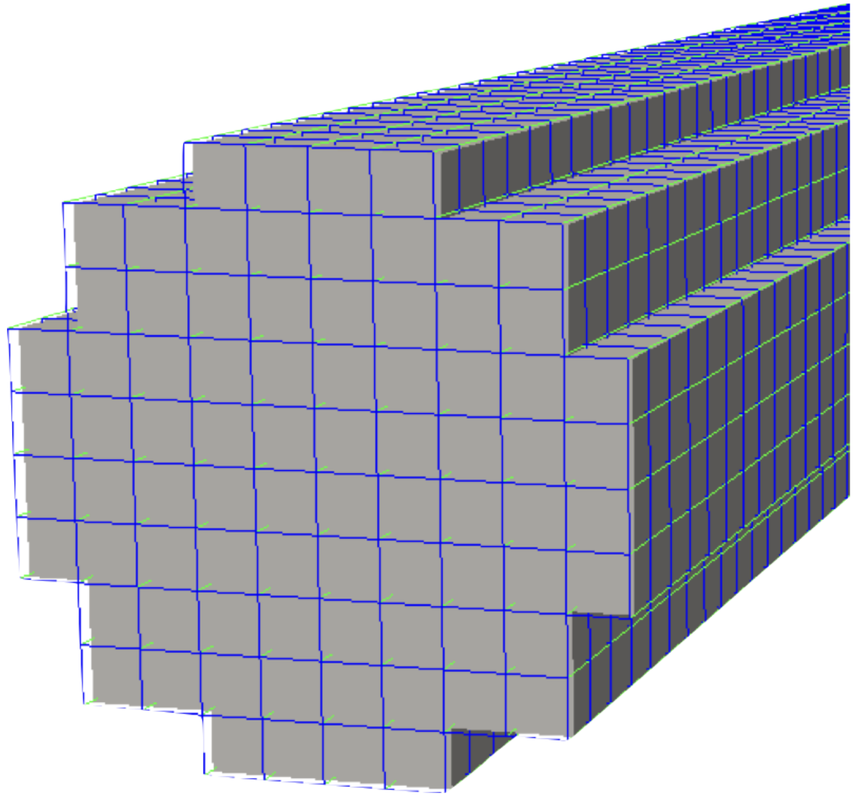

Automatic dielectric smoothing at Yee cell boundaries

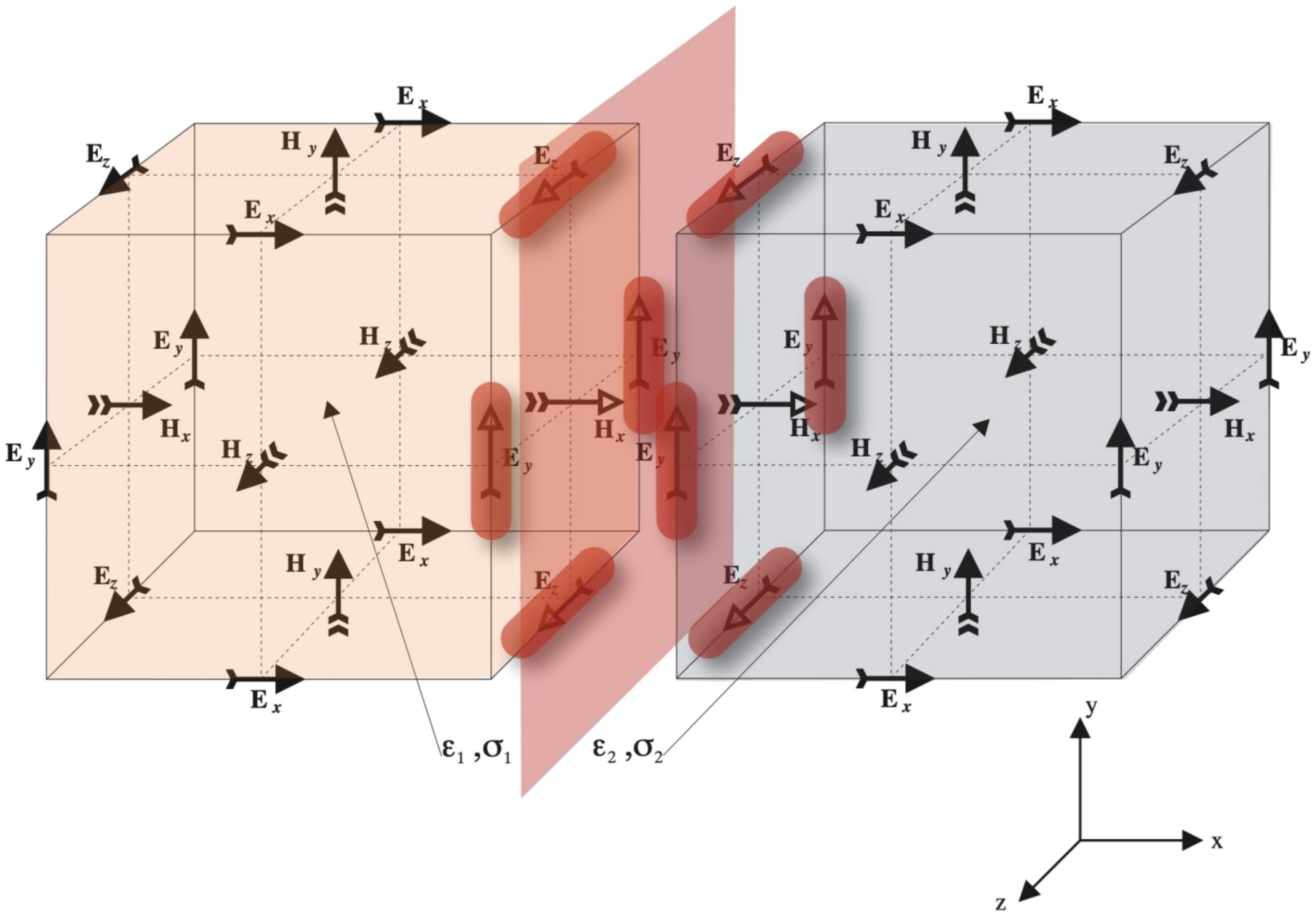

Soil or complex structure modelling: Stochastically distributed frequency depended properties of soils based on the Peplinski model

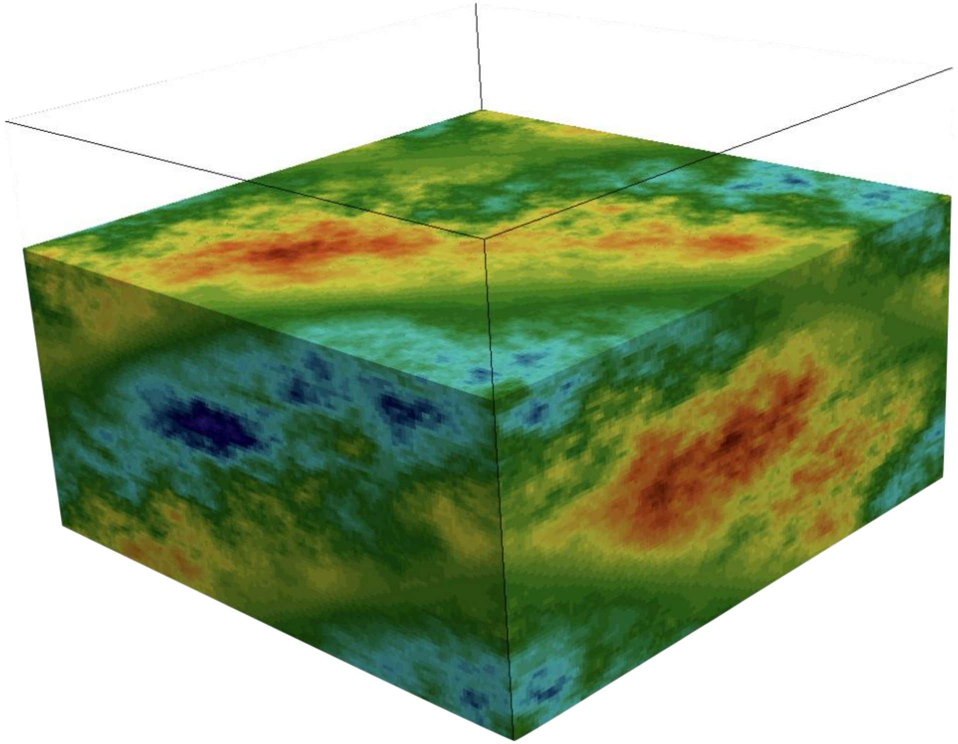

Giannakis, I., Giannopoulos, A., & Warren, C. (2016), "A Realistic FDTD Numerical Modeling Framework of Ground Penetrating Radar for Landmine Detection", **IEEE Journal of Selected Topics in Applied Earth Observations and Remote Sensing**, 9(1), 37-51

epcc

Stochastic distribution of material properties, including rough surfaces, water puddles and even blades of grass!

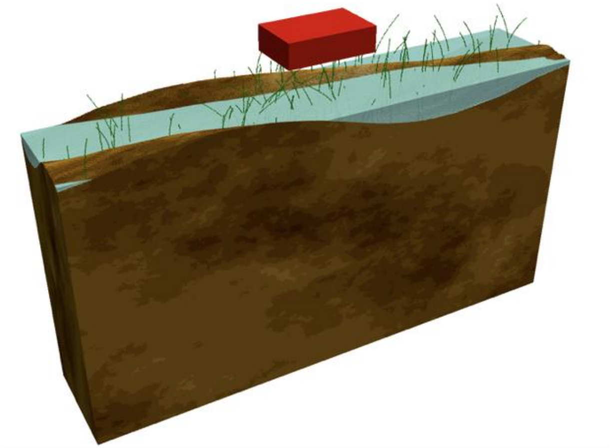

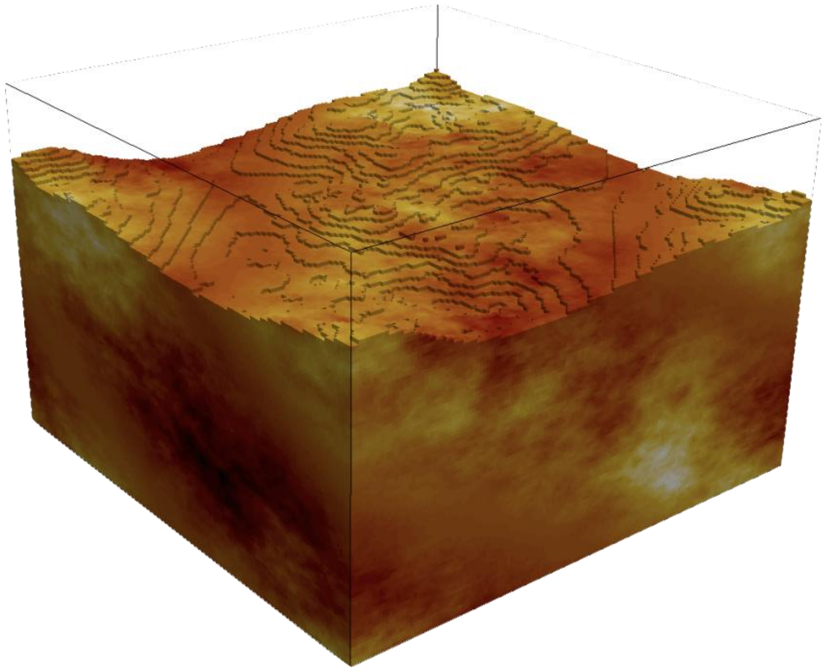

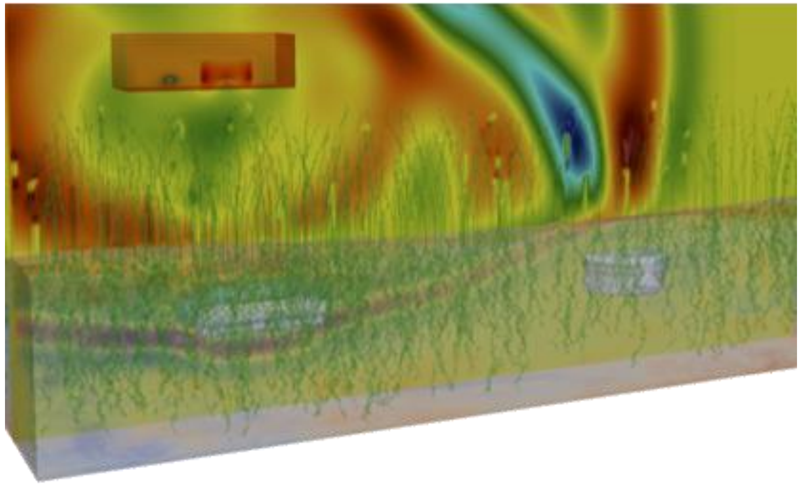

Biomedical EM modelling

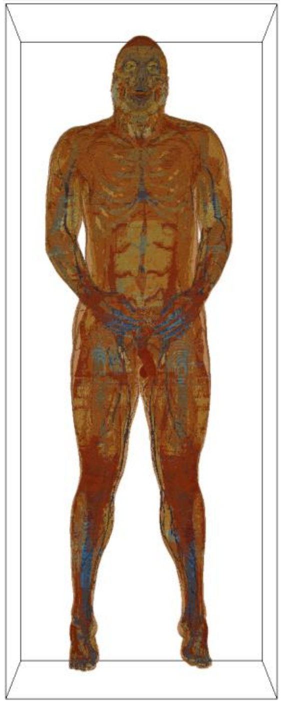

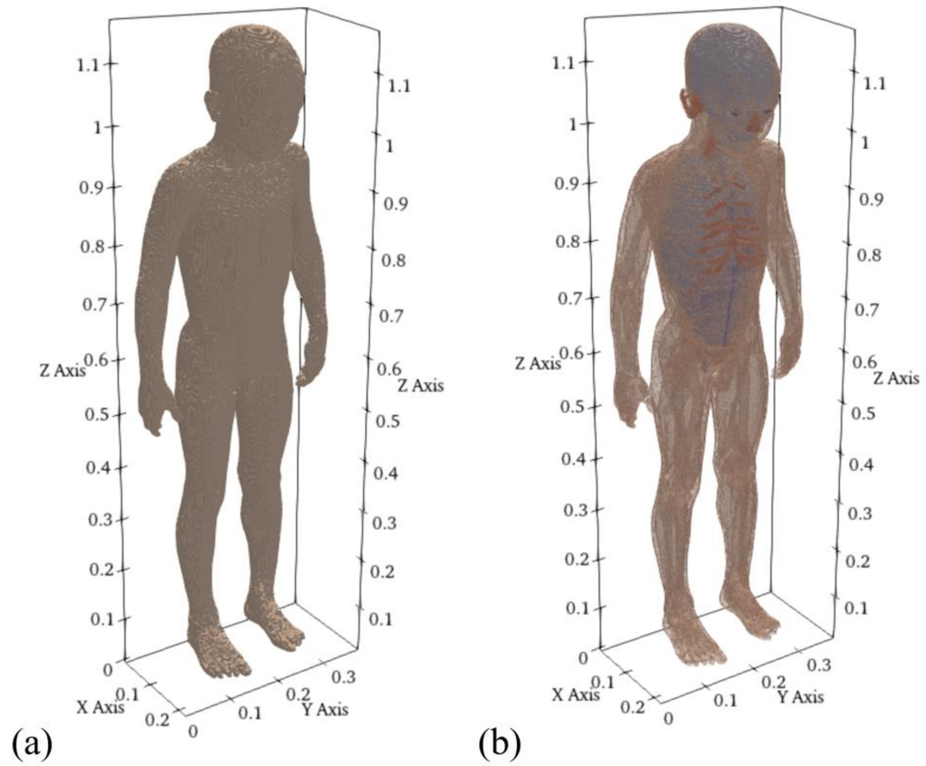

https://itis.swiss/virtual-population/virtual-population/overview/

https://web.corral.tacc.utexas.edu/AustinManEMVoxels/AustinMan/index.html

Massey, J., Geyik, C., Techachainiran, N., Hsu, C., Nguyen, R., Latson, T., Ball, M. & Yilmaz, A. (2012), "AustinMan and AustinWoman: High fidelity, reproducible, and open-source electromagnetic voxel models," in Proc. Bioelectromagnetics Soc. 34th Annual Meeting

Simple example

Please look up the detailed documentation where you can find examples!

Half-wavelength wire dipole antenna in free space

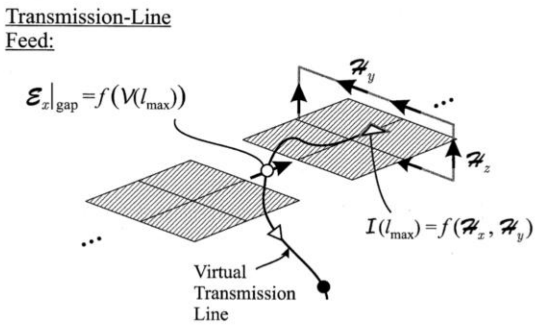


```
#title: Wire antenna - half-wavelength dipole in free-space
#domain: 0.050 0.050 0.200
#dx_dy_dz: 0.001 0.001 0.001
#time_window: 60e-9

#waveform: gaussian 1 1e9 mypulse
#transmission_line: z 0.025 0.025 0.100 73 mypulse

## 150mm length
#edge: 0.025 0.025 0.025 0.025 0.025 0.175 pec
## 1mm gap at centre of dipole
#edge: 0.025 0.025 0.100 0.025 0.025 0.101 free_space
#geometry_view: 0.020 0.020 0.020 0.030 0.030 0.180 0.001 0.001 0.001 antenna_wire_dipole_fs f
```

Half-wavelength wire dipole antenna in free space

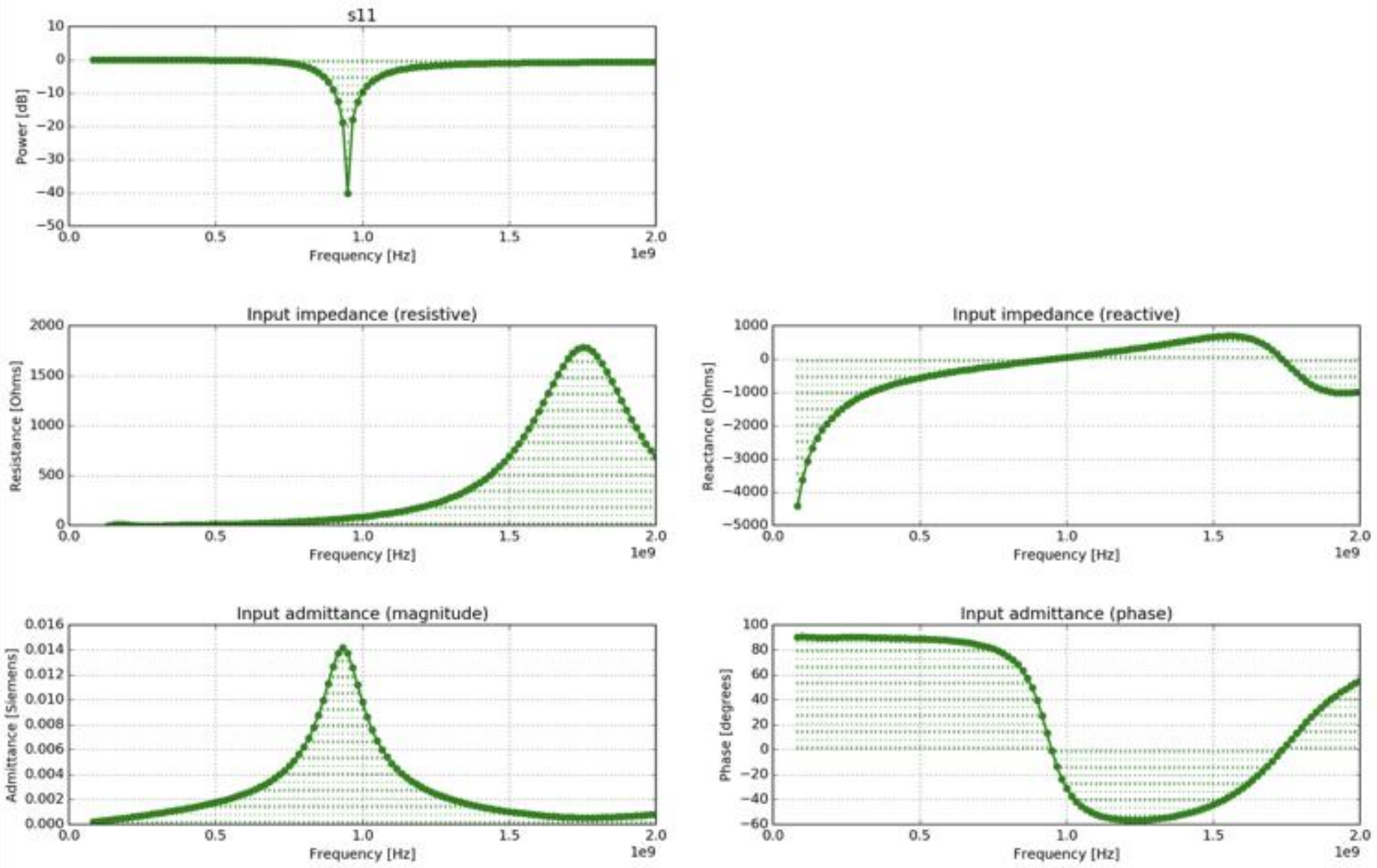

Wire dipole antenna over a half-space

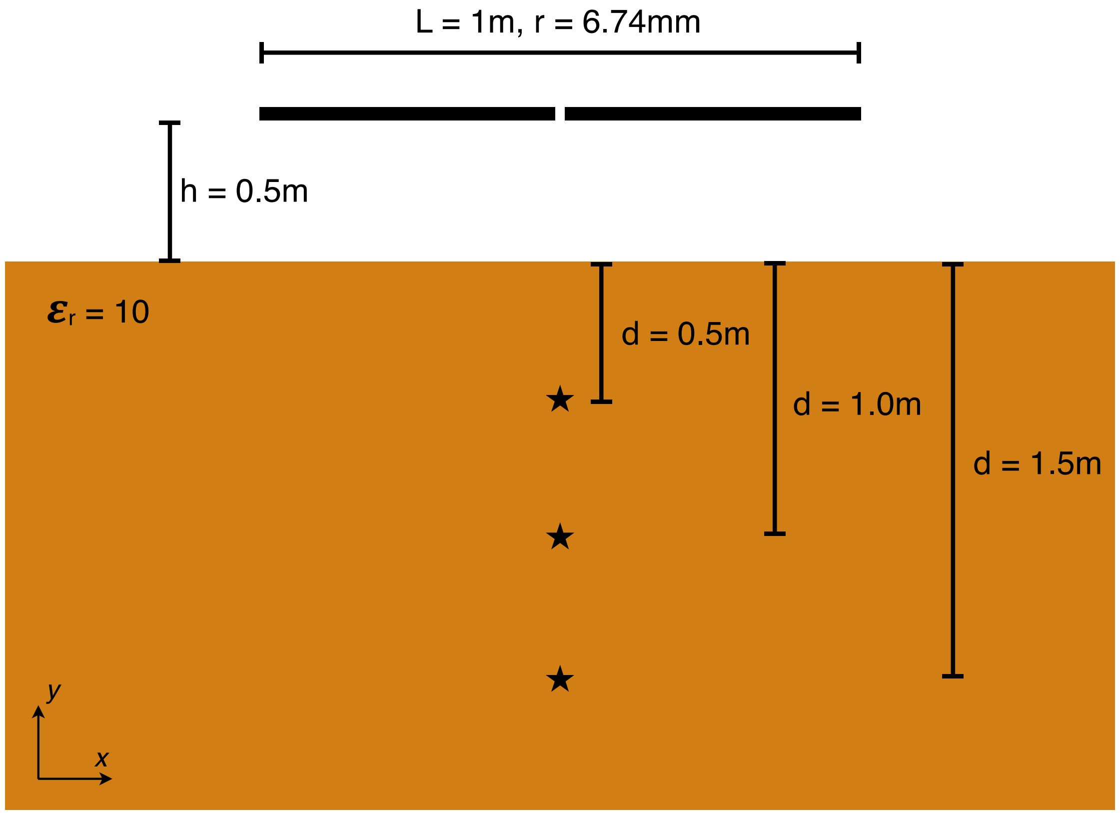

$$V(t) = V_0 e^{-g^2(t-t_0)^2},$$
$$V_0 = 1 \text{ V}$$
$$g = 1.5 \times 10^9$$
$$t_0 = 1.43 \times 10^{-9} \text{ s}$$

$$\Delta x = \Delta y = \Delta z = 10 \text{ mm}$$
$$f_c = 337 \text{ MHz}$$

Ix@ feed

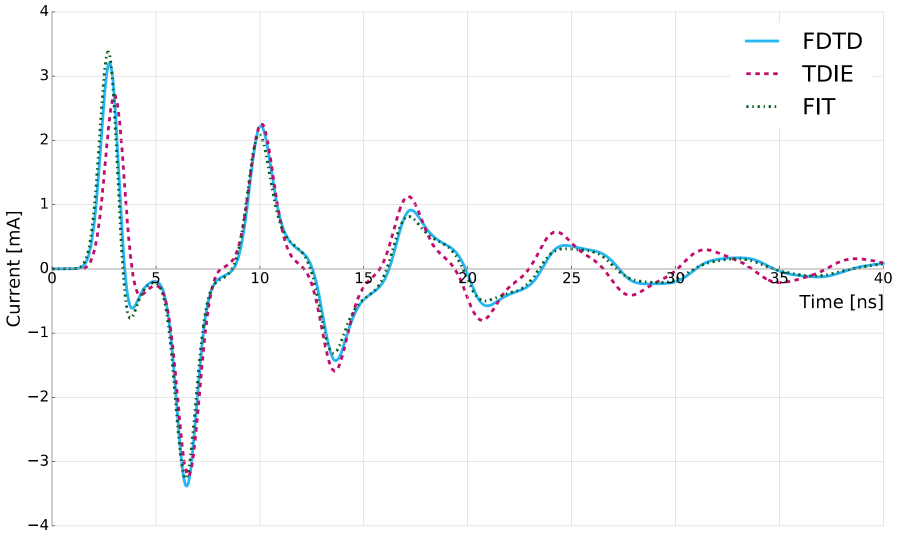

Ex@ d=0.5m

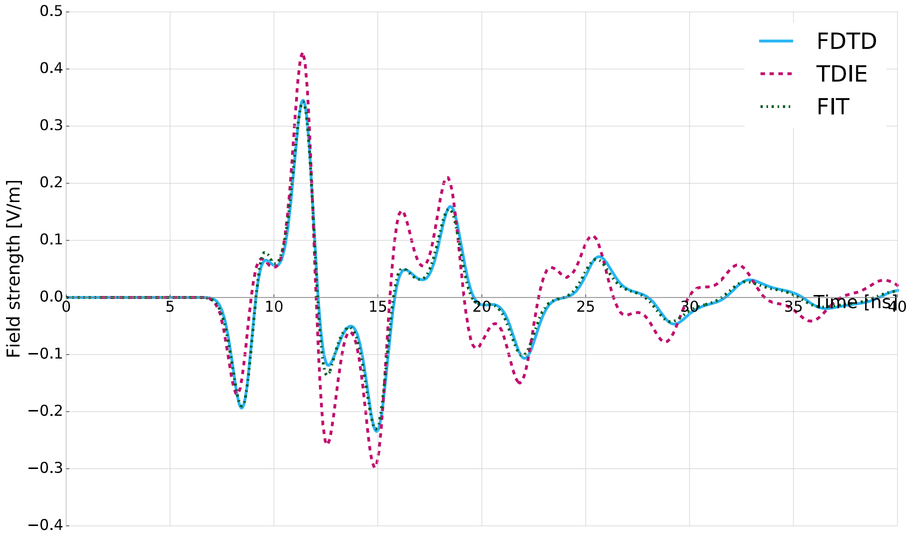

Ex@ d=1.0m

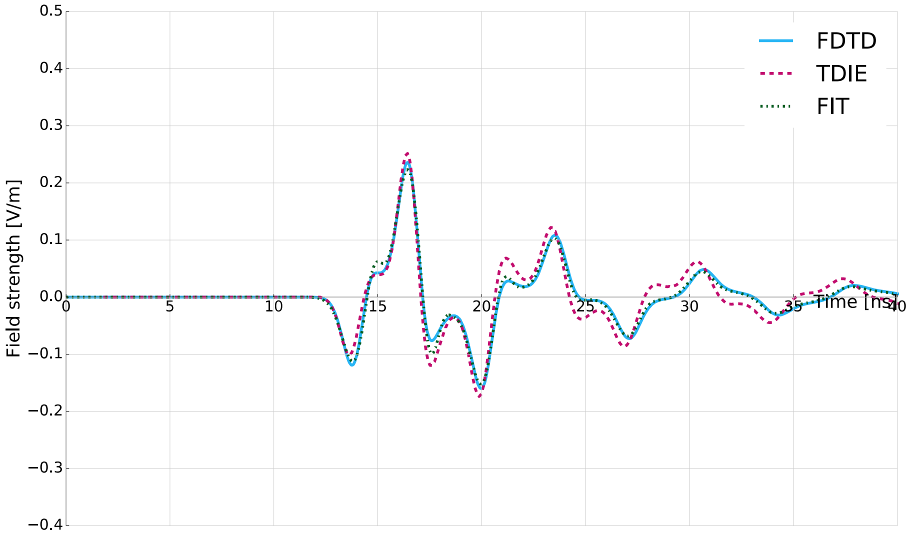

Ex@ d=1.5m

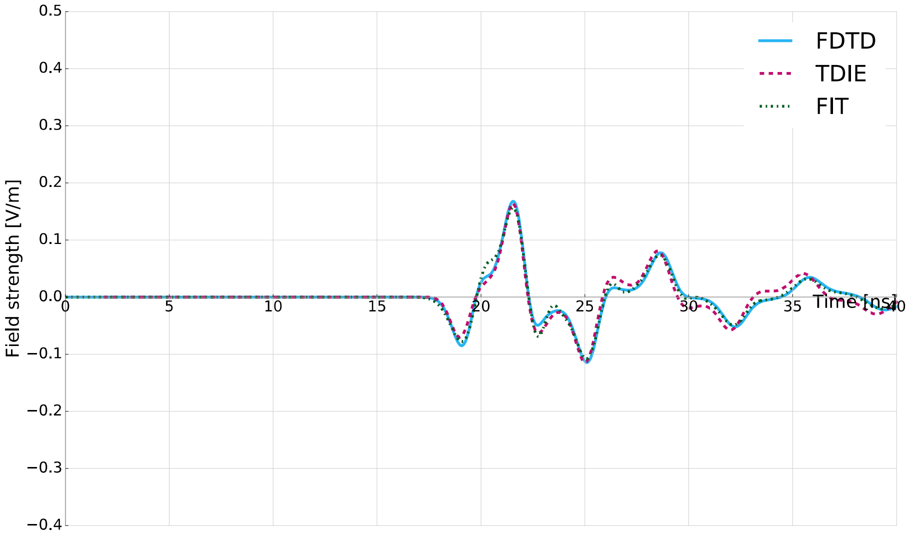

Modelling GPR transducers

Commercial GPR antennas

GSSI 1.5GHz antenna

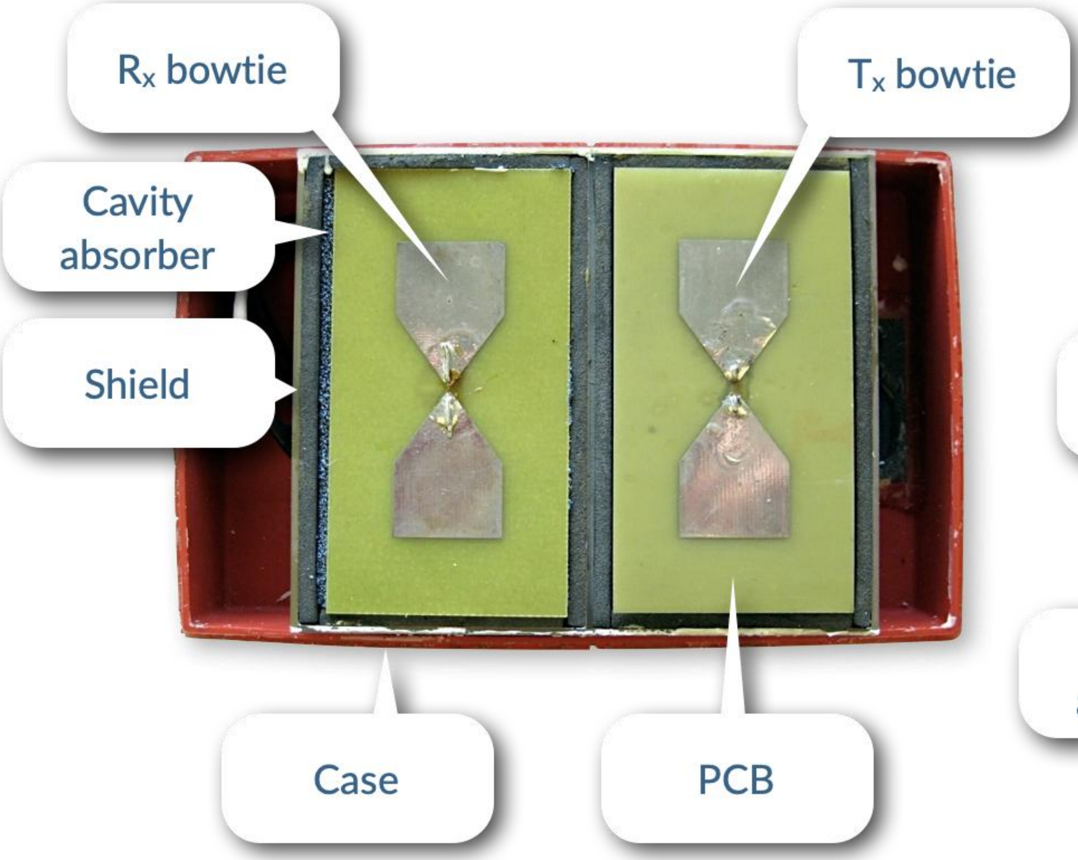

MALÅ 1.2GHz antenna

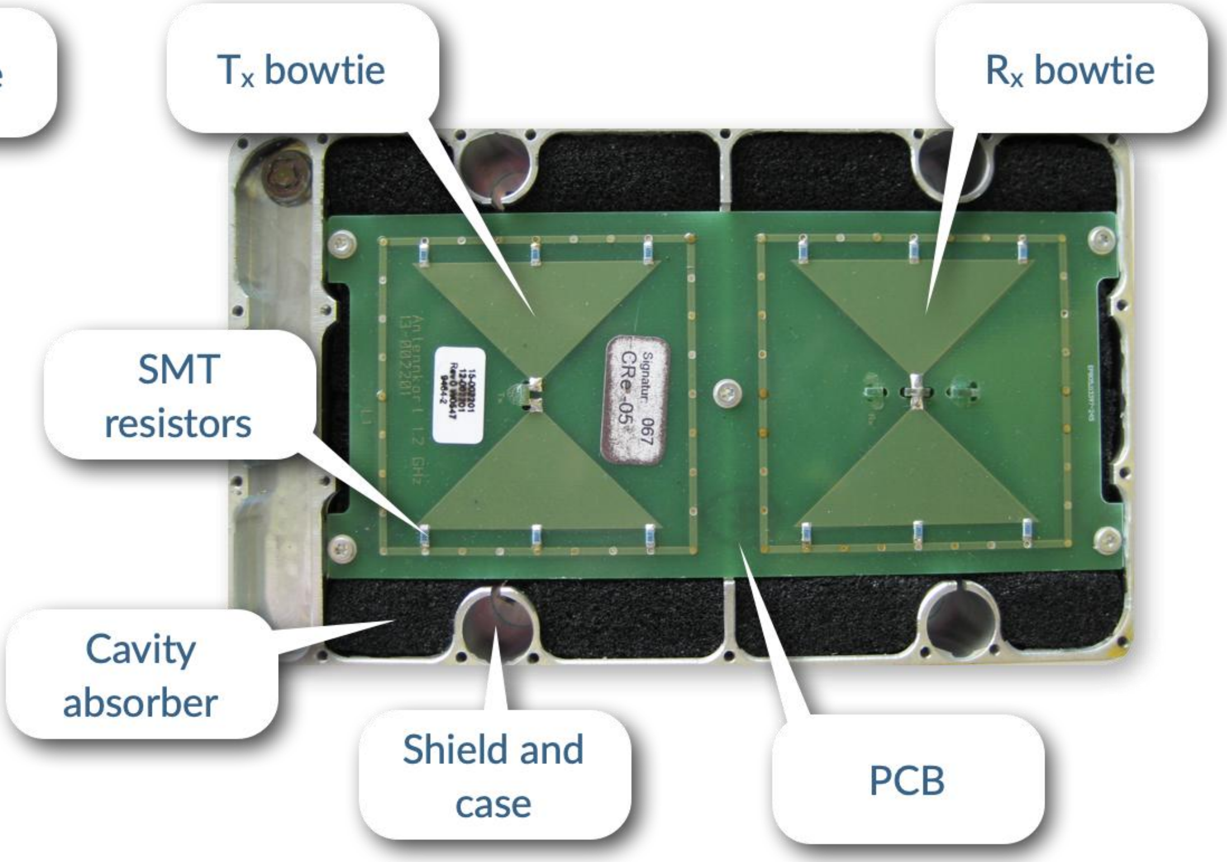

FDTD antenna models of commercial GPR antennas

GSSI 1.5GHz antenna

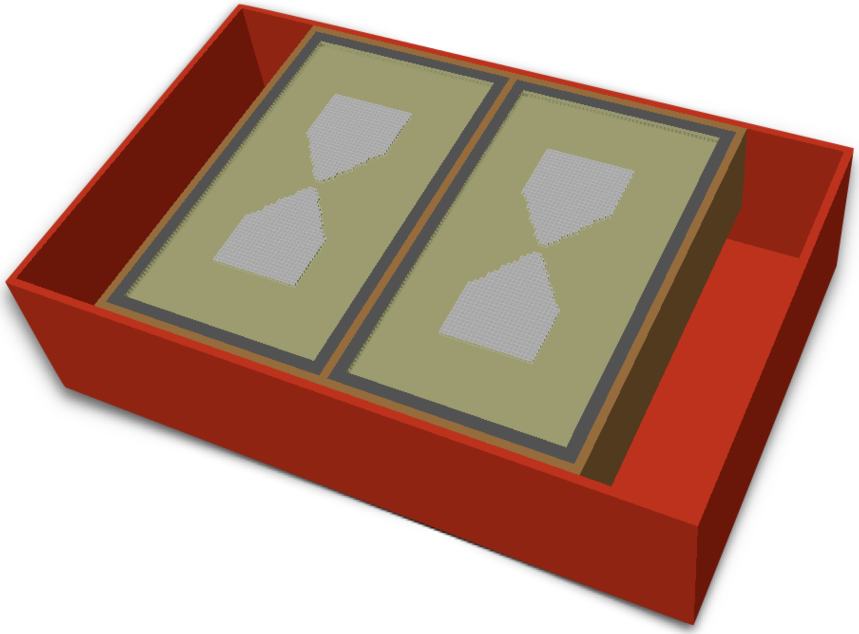

MALA 1.2GHz antenna

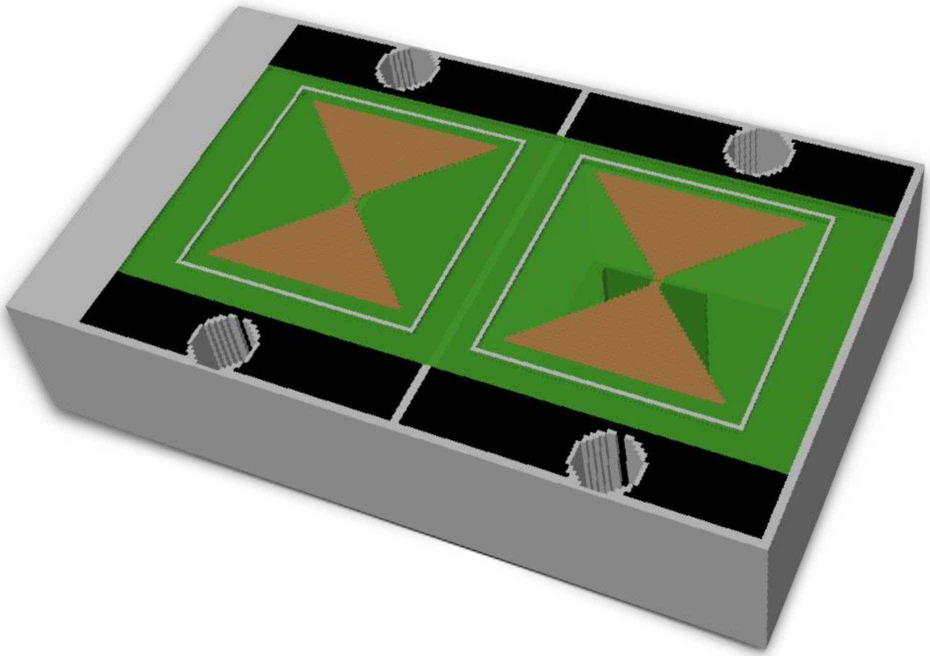

Warren, C. & Giannopoulos, A. (2011) Creating finite-difference time-domain models of commercial ground-penetrating radar antennas using Taguchi's optimization method, **Geophysics**, 76(2), G37-G47

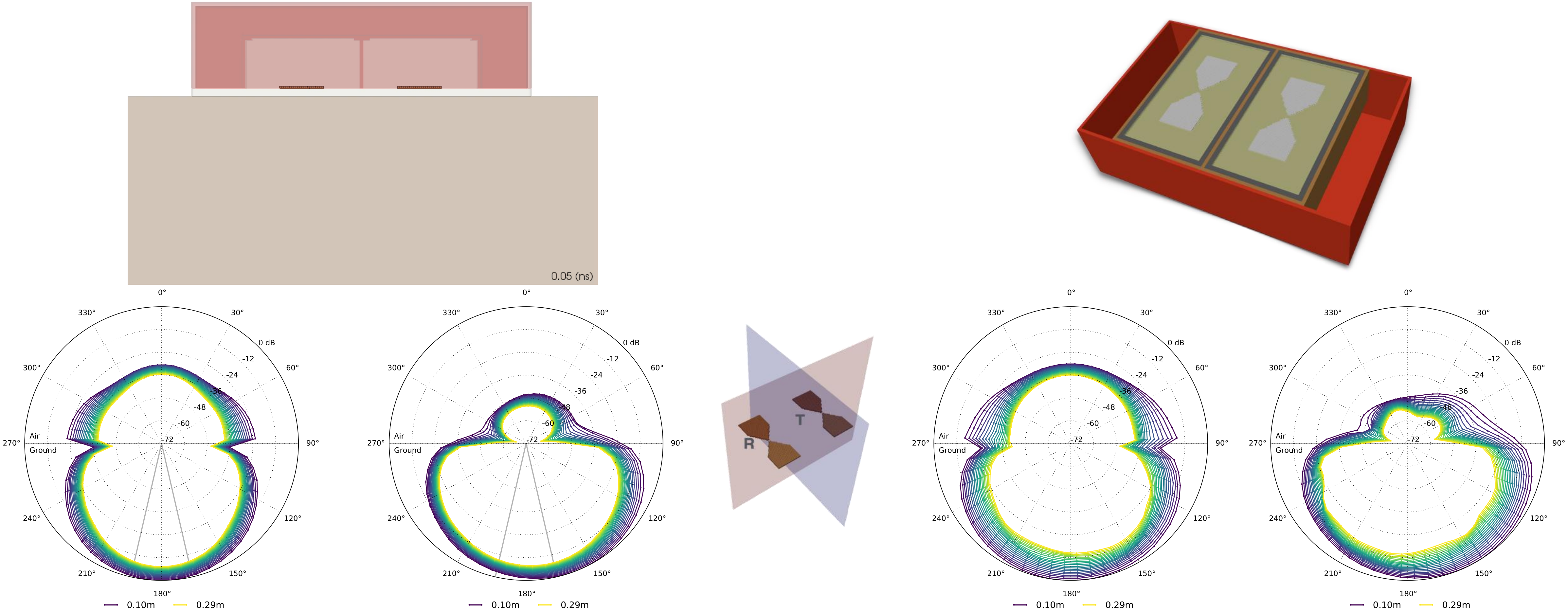

Warren C. and Giannopoulos A., (2017) Characterisation of Ground Penetrating Radar antenna in Lossless Homogeneous and Lossy Heterogeneous Environments, Signal Processing, 132, pp. 221-226

FDTD antenna models of commercial GPR antennas

GSSI 1.5GHz antenna

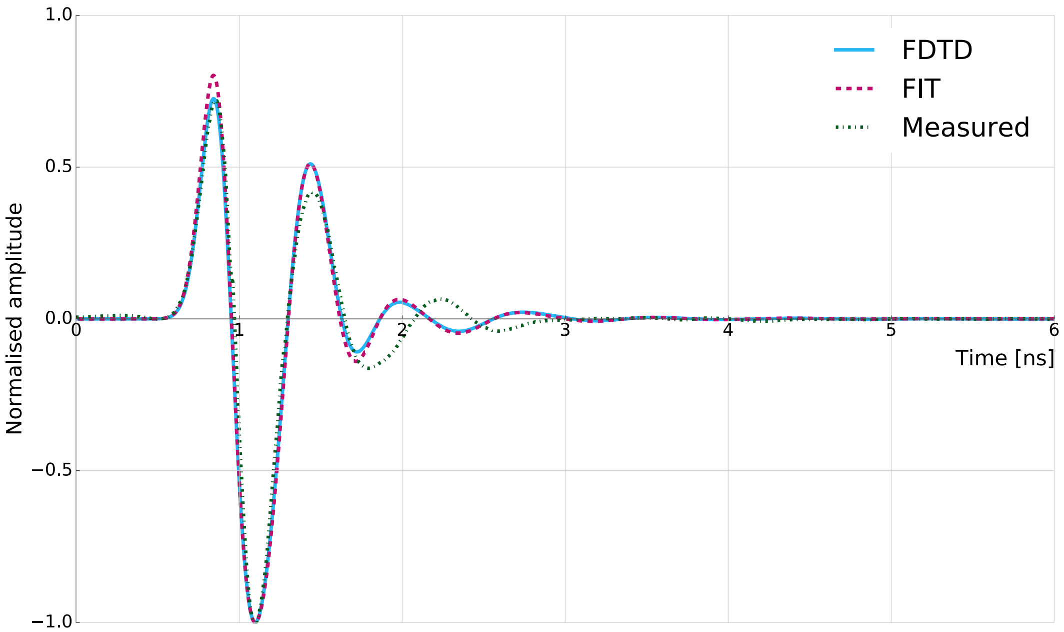

MALA 1.2GHz antenna

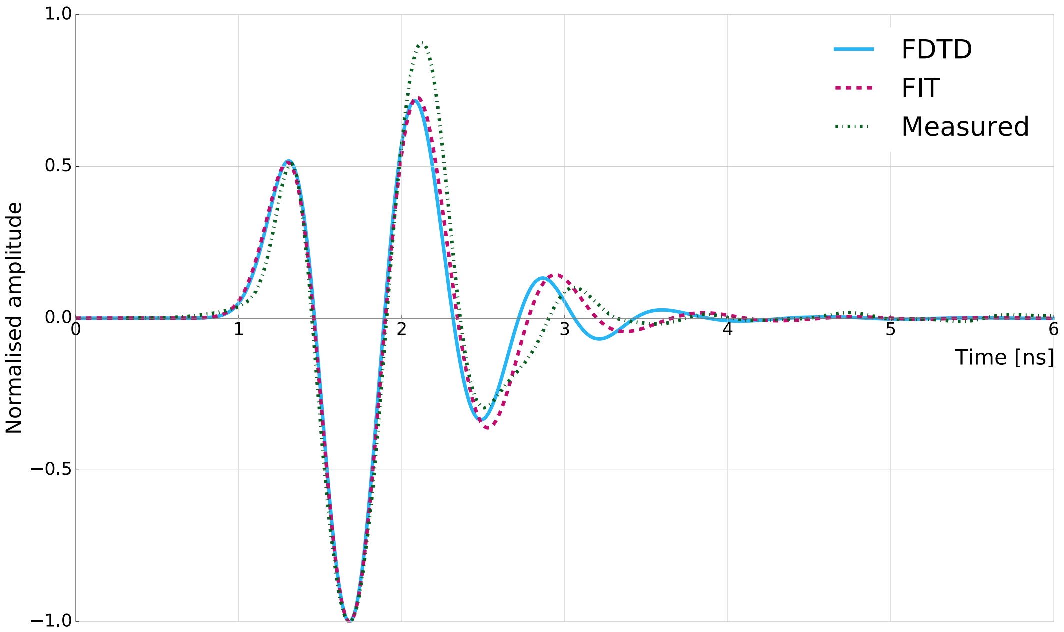

epcc

Advanced applications

GPR – Advanced data processing and Machine Learning

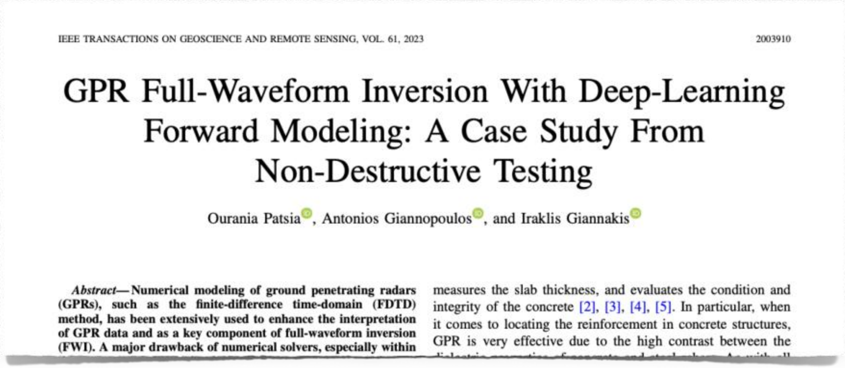

IEEE TRANSACTIONS ON GEOSCIENCE AND REMOTE SENSING, VOL. 61, 2023 2003910

GPR Full-Waveform Inversion With Deep-Learning Forward Modeling: A Case Study From Non-Destructive Testing

Ourania Patsia, Antonios Giannopoulos, and Iraklis Giannakis

Abstract—Numerical modeling of ground penetrating radars (GPRs), such as the finite-difference time-domain (FDTD) method, has been extensively used to enhance the interpretation of GPR data and as a key component of full-waveform inversion (FWI). A major drawback of numerical solvers, especially within

measures the slab thickness, and evaluates the condition and integrity of the concrete [2], [3], [4], [5]. In particular, when it comes to locating the reinforcement in concrete structures, GPR is very effective due to the high contrast between the

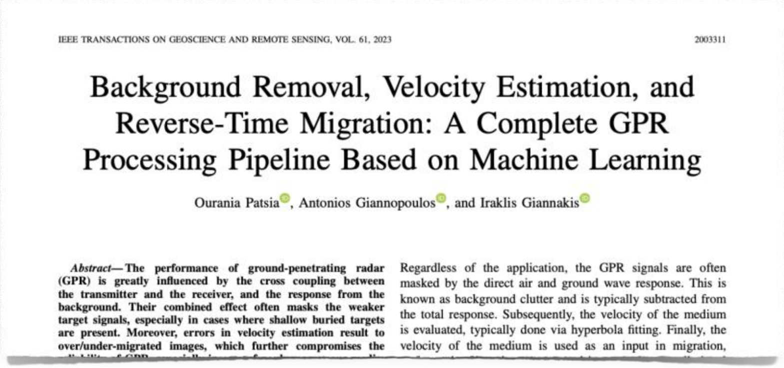

IEEE TRANSACTIONS ON GEOSCIENCE AND REMOTE SENSING, VOL. 61, 2023 2003311

Background Removal, Velocity Estimation, and Reverse-Time Migration: A Complete GPR Processing Pipeline Based on Machine Learning

Ourania Patsia, Antonios Giannopoulos, and Iraklis Giannakis

Abstract—The performance of ground-penetrating radar (GPR) is greatly influenced by the cross coupling between the transmitter and the receiver, and the response from the background. Their combined effect often masks the weaker target signals, especially in cases where shallow buried targets are present. Moreover, errors in velocity estimation result to over/under-migrated images, which further compromises the

Regardless of the application, the GPR signals are often masked by the direct air and ground wave response. This is known as background clutter and is typically subtracted from the total response. Subsequently, the velocity of the medium is evaluated, typically done via hyperbola fitting. Finally, the velocity of the medium is used as an input in migration,

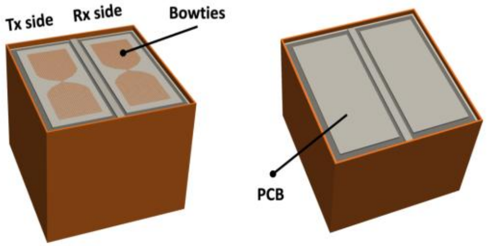

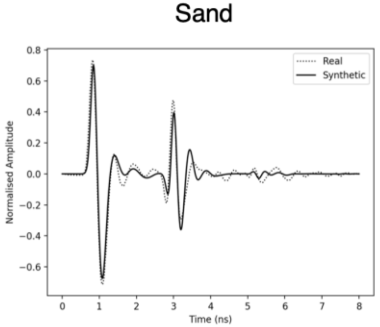

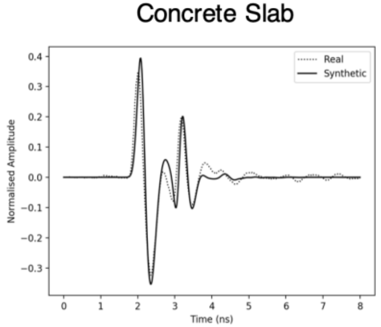

Reverse time migration using an ML predicted permittivity distribution

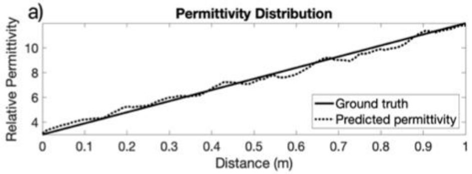

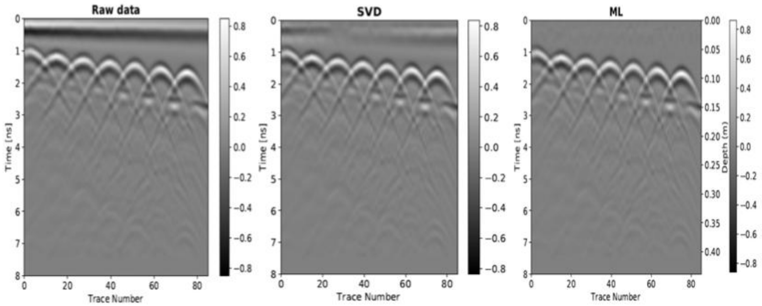

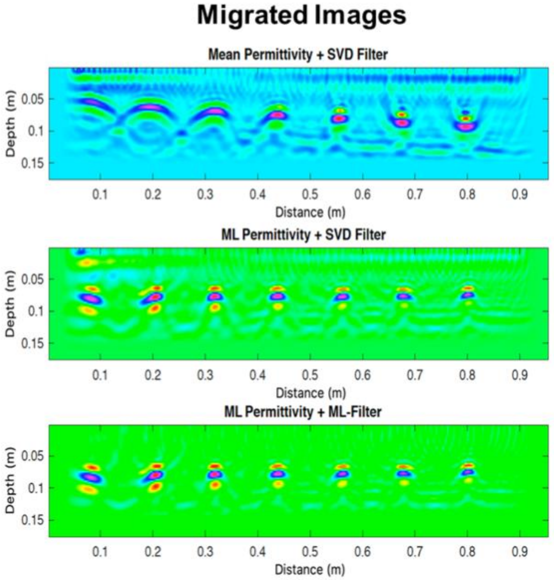

GPR - Landmines

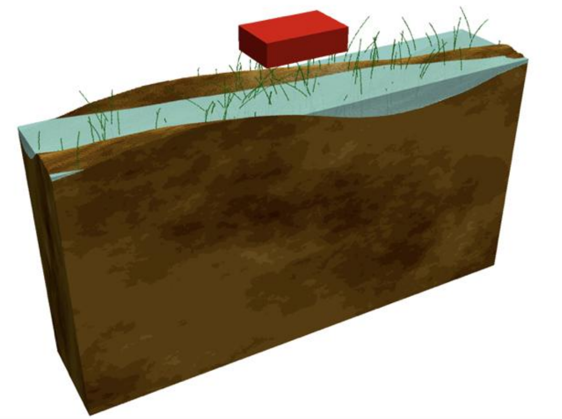

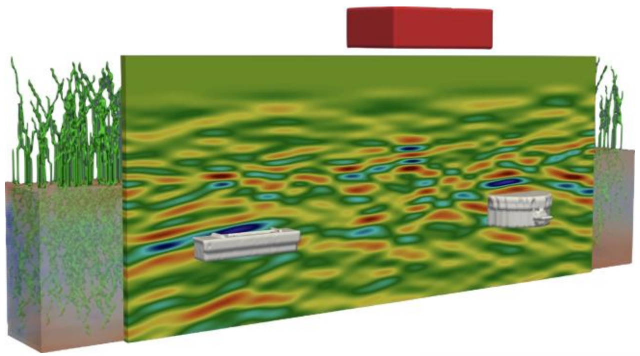

IEEE JOURNAL OF SELECTED TOPICS IN APPLIED EARTH OBSERVATIONS AND REMOTE SENSING, VOL. 9, NO. 1, JANUARY 2016 37

A Realistic FDTD Numerical Modeling Framework of Ground Penetrating Radar for Landmine Detection

Iraklis Giannakis, Antonios Giannopoulos, and Craig Warren

***Abstract*—A three-dimensional (3-D) finite-difference time-domain (FDTD) algorithm is used in order to simulate ground penetrating radar (GPR) for landmine detection. Two bowtie GPR transducers are chosen for the simulations and two widely employed antipersonnel (AP) landmines, namely PMA-1 and PMN are used. The validity of the modeled antennas and landmines is tested through a comparison between numerical and laboratory measurements. The modeled AP landmines are buried in a realistically simulated soil. The geometrical characteristics of soil's inhomogeneity are modeled using fractal correlated noise, which gives rise to Gaussian semivariograms often encountered in the field. Fractals are also employed in order to simulate the**

A better understanding of the scattering mechanisms within the ground can help us increase the effectiveness of GPR and investigate its limitations. This can be achieved through numerical modeling that can provide insight on how the soil's characteristics can influence the overall performance of GPR. Apart from that, numerical modeling can be a practical tool for testing and comparing different antennas and processing algorithms in a wide range of environments. Furthermore, a realistic numerical model can also be employed for training purposes in machine learning based approaches. In order to address

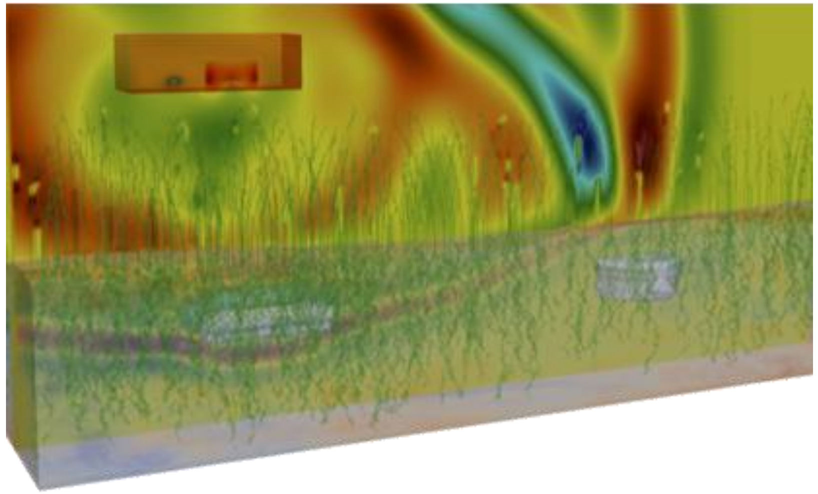

GPR – Planetary

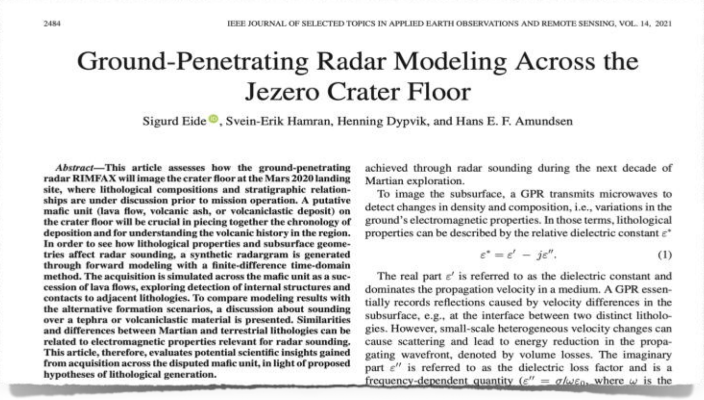

Ground-Penetrating Radar Modeling Across the Jezero Crater Floor

Sigurd Eide, Svein-Erik Hamran, Henning Dypvik, and Hans E. F. Amundsen

Abstract—This article assesses how the ground-penetrating radar RIMFAX will image the crater floor at the Mars 2020 landing site, where lithological compositions and stratigraphic relationships are under discussion prior to mission operation. A putative mafic unit (lava flow, volcanic ash, or volcaniclastic deposit) on the crater floor will be crucial in piecing together the chronology of deposition and for understanding the volcanic history in the region. In order to see how lithological properties and subsurface geometries affect radar sounding, a synthetic radargram is generated through forward modeling with a finite-difference time-domain method. The acquisition is simulated across the mafic unit as a succession of lava flows, exploring detection of internal structures and contacts to adjacent lithologies. To compare modeling results with the alternative formation scenarios, a discussion about sounding over a tephra or volcaniclastic material is presented. Similarities and differences between Martian and terrestrial lithologies can be related to electromagnetic properties relevant for radar sounding. This article, therefore, evaluates potential scientific insights gained from acquisition across the disputed mafic unit, in light of proposed hypotheses of lithological generation.

achieved through radar sounding during the next decade of Martian exploration.

To image the subsurface, a GPR transmits microwaves to detect changes in density and composition, i.e., variations in the ground's electromagnetic properties. In those terms, lithological properties can be described by the relative dielectric constant ε^*

$$\varepsilon^* = \varepsilon' - j\varepsilon''. \quad (1)$$

The real part ε' is referred to as the dielectric constant and dominates the propagation velocity in a medium. A GPR essentially records reflections caused by velocity differences in the subsurface, e.g., at the interface between two distinct lithologies. However, small-scale heterogeneous velocity changes can cause scattering and lead to energy reduction in the propagating wavefront, denoted by volume losses. The imaginary part ε'' is referred to as the dielectric loss factor and is a frequency-dependent quantity ($\varepsilon'' = \sigma/\omega\varepsilon_0$, where ω is the


Hindawi
International Journal of Antennas and Propagation
Volume 2017, Article ID 3013249, 11 pages
https://doi.org/10.1155/2017/3013249

Research Article

Numerical Simulations of the Lunar Penetrating Radar and Investigations of the Geological Structures of the Lunar Regolith Layer at the Chang'E 3 Landing Site

Chunyu Ding,[1,2,3] Yan Su,[1,2] Shuguo Xing,[1,2] Shun Dai,[1,2] Yuan Xiao,[1,2,3] Jianqing Feng,[1,2] Danqing Liu,[4] and Chunlai Li[1,2]

[1]Key Laboratory of Lunar and Deep Space Exploration, Chinese Academy of Sciences, Beijing 100012, China
[2]National Astronomical Observatories, Chinese Academy of Sciences, Beijing 100012, China
[3]University of Chinese Academy of Sciences, Beijing 100049, China
[4]Renmin University of China, Beijing 100872, China

Correspondence should be addressed to Yan Su; suyan@nao.cas.cn

Received 21 December 2016; Revised 12 March 2017; Accepted 3 April 2017; Published 23 May 2017

Academic Editor: Han Guo

In the process of lunar exploration, and specifically when studying lunar surface structure and thickness, the established lunar regolith model is usually a uniform and ideal structural model, which is not well-suited to describe the real structure of the lunar regolith layer. The present study aims to explain the geological structural information contained in the channel 2 LPR (lunar penetrating radar) data. In this paper, the random medium theory and Apollo drilling core data are used to construct

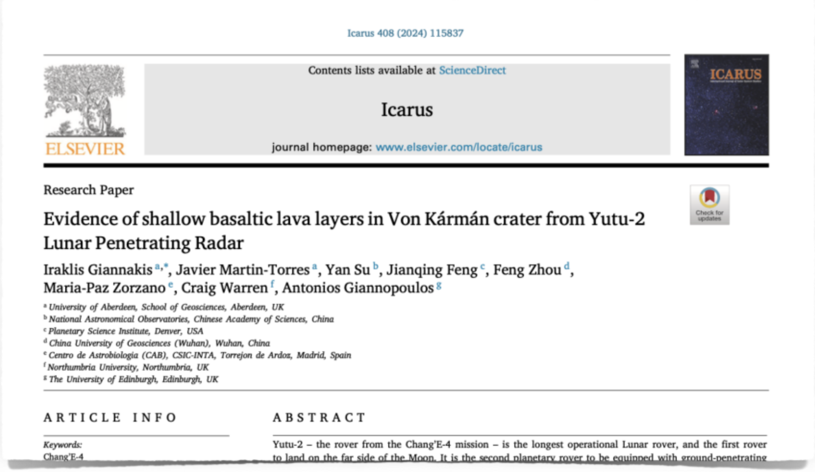
Icarus 408 (2024) 115837

Contents lists available at ScienceDirect

Icarus

journal homepage: www.elsevier.com/locate/icarus

Research Paper

Evidence of shallow basaltic lava layers in Von Kármán crater from Yutu-2 Lunar Penetrating Radar

Iraklis Giannakis [a,*], Javier Martin-Torres [a], Yan Su [b], Jianqing Feng [c], Feng Zhou [d], Maria-Paz Zorzano [e], Craig Warren [f], Antonios Giannopoulos [g]

[a] University of Aberdeen, School of Geosciences, Aberdeen, UK
[b] National Astronomical Observatories, Chinese Academy of Sciences, China
[c] Planetary Science Institute, Denver, USA
[d] China University of Geosciences (Wuhan), Wuhan, China
[e] Centro de Astrobiologia (CAB), CSIC-INTA, Torrejon de Ardoz, Madrid, Spain
[f] Northumbria University, Northumbria, UK
[g] The University of Edinburgh, Edinburgh, UK

ARTICLE INFO

Keywords:
Chang'E-4

ABSTRACT

Yutu-2 – the rover from the Chang'E-4 mission – is the longest operational Lunar rover, and the first rover to land on the far side of the Moon. It is the second planetary rover to be equipped with ground-penetrating

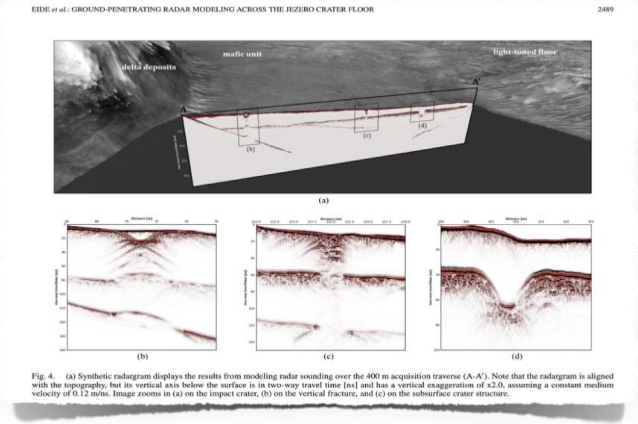

Fig. 4. (a) Synthetic radargram displays the results from modeling radar sounding over the 400 m acquisition traverse (A-A'). Note that the radargram is aligned with the topography, but its vertical axis below the surface is in two-way travel time [ns] and has a vertical exaggeration of x2.0, assuming a constant medium velocity of 0.12 m/ns. Image zooms in (a) on the impact crater, (b) on the vertical fracture, and (c) on the subsurface crater structure.

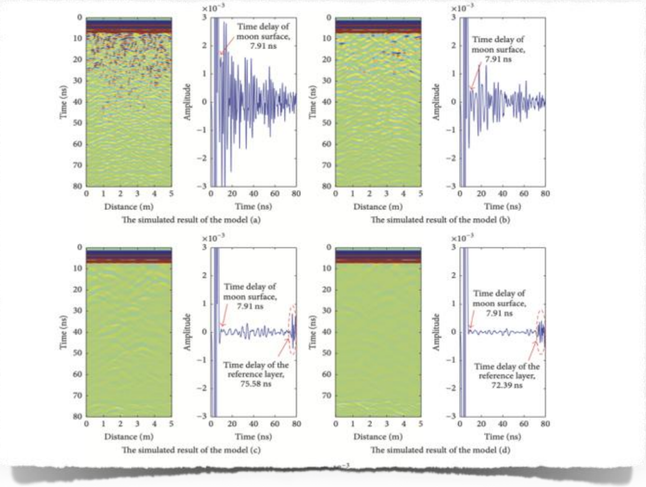

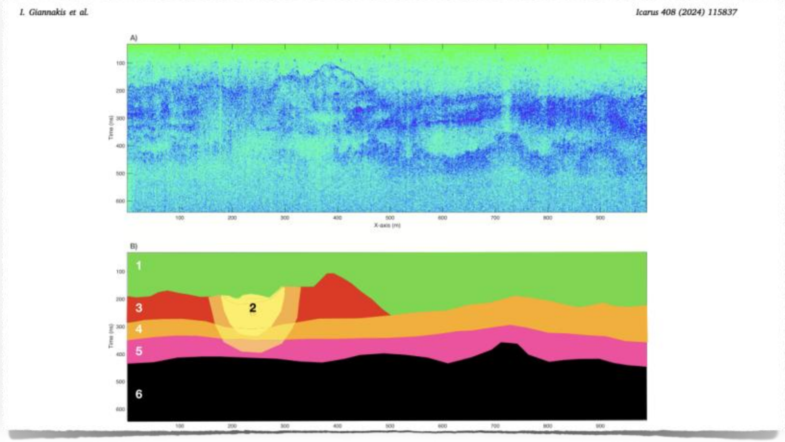

epcc

Now and the future of gprMax

Google
Summer of Code

We participated in GSoC in 2019, 2021, 2023, 2024 and in 2025

Google Summer of Code

LibreCube Initiative
Open Source Space Exploration

Open Chemistry
Advancing Open Source & Open Science for Chemistry

CGAL Project
C++ library of computational geometry

SageMath
Open-source mathematics software system

INCF
An open & FAIR neuroscience standards organization

GNSS-SDR
An open source GNSS software-defined receiver

caMicroscope
Toolkit for cancer imaging research

gprMax
Simulating electromagnetic wave propagation

GNU Radio
The free & open software radio ecosystem

DeepChem
Democratize AI for drug discovery.

Python Software Foundation
A programming language used for science & more

GNU Octave
Free Your Numbers

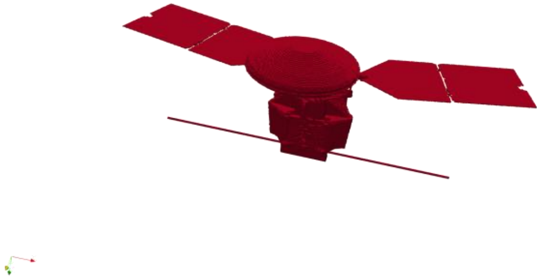

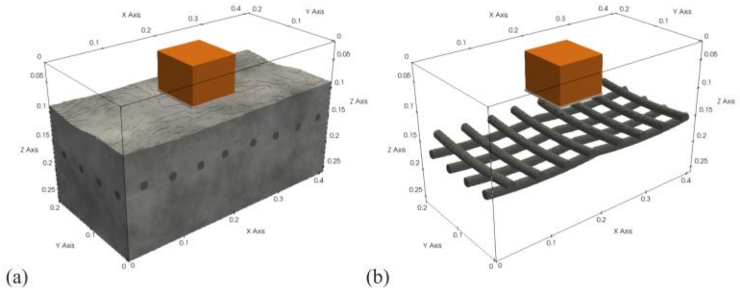

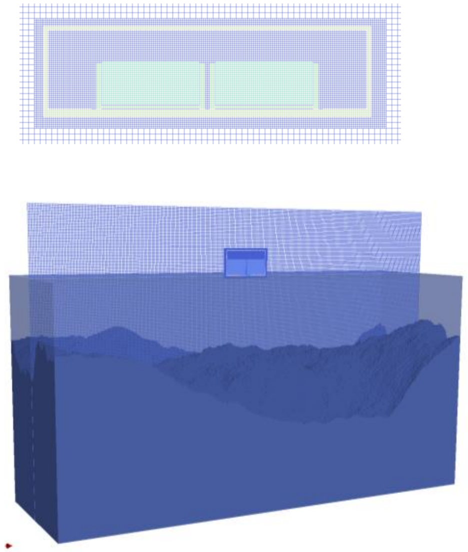

Next version of gprMax - beta testing 18-Jul-2023

We are almost ready to release the next version of gprMax (v4) code named Carn Mor, continuing our single malt Scotch whisky theming! Carn Mor has a number of new and exciting features such as:

- **Sub-gridding** - the ability to define different spatial resolutions in different areas of the main grid. This allows high-dielectric materials and fine geometries to be more efficiently modelled.
- **OpenCL support** - run your simulations more quickly on hardware (CPU and GPU) that supports OpenCL.
- **STLtoVoxel toolbox** - convert STL files and import complex geometries without having to build them from geometry commands.
- **DebyeFit toolbox** - simulate materials with dispersive properties described by relaxation models such as Havriliak-Negami, Jonscher, Complex Refractive Index Mixing (CRIM), or your own measured data.
- **Landmine toolbox** - contains realistic models of anti-personnel (AP) landmines including the PMA-1, PMN, and TS-50.

There are many more new features and also lots of under-the-hood improvements. **We are seeking current gprMax users to beta test this new version which is available through the devel branch on our GitHub repository**. Please report bugs through our GitHub issue tracker and use the tag *v4 bug*.

eCSE project:

Large-scale open-source computational electrodynamics:
MPI domain decomposition for gprMax

Why MPI domain decomposition?

- Maximum model size on a single node of ARCHER2 (256GB memory):
  - 1.6m x 1.6m x 1.6m model at 1mm resolution
  - 4.096m^3 or 4.096×10^9 cells

- Using more complex geometry increases memory usage
- Taking snapshots can increase memory usage

Why MPI domain decomposition?

- Existing gprMax solvers:
  - CPU (OpenMP)
  - GPU (CUDA)
  - OpenCL
- All of these solvers are limited to a single node or device
- To run larger simulations, we need more memory

- HPC systems do have nodes with large amounts of memory, but:
  - Limit to OpenMP scaling within a node
  - MPI scales beyond a single node (and hopefully adds performance too)

Adding MPI domain decomposition

- Minimal changes for users – no need to change the model definition
- Control decomposition using the new `--mpi` flag

```
$ mpirun -n 8 python -m gprMax model.in --mpi 2 2 2
```

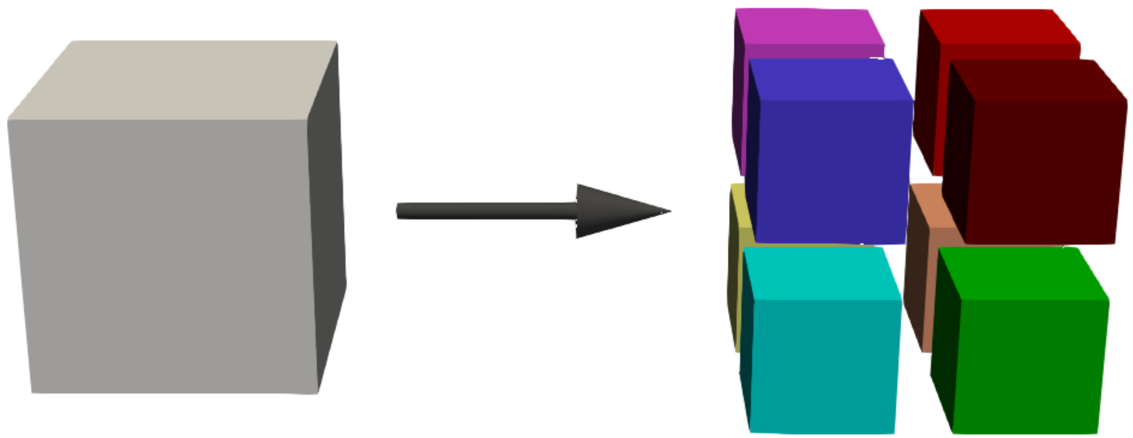

Solver Loop

- Simplified control flow of the main solver

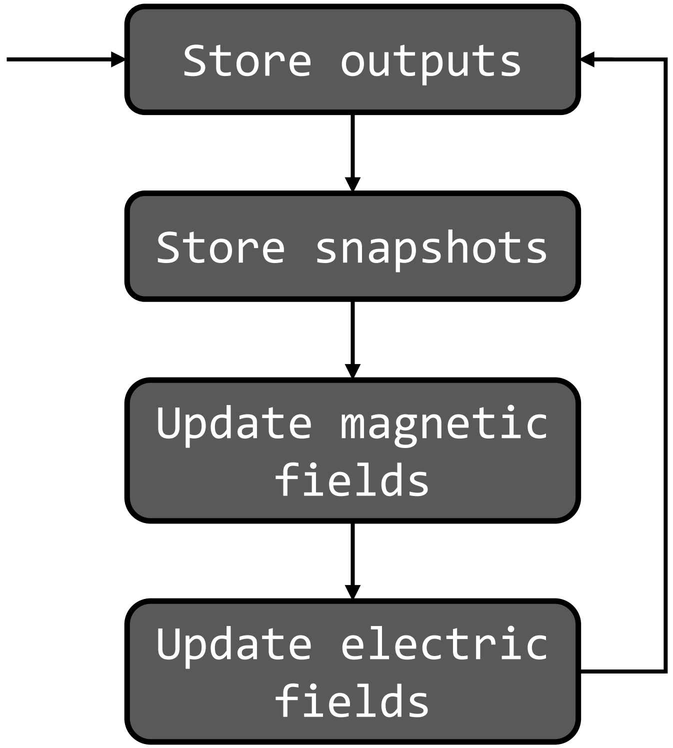

Solver Loop

- Simplified control flow of the main solver
- Addition of halo exchanges
  - Direct point to point communication with neighbours
  - Asynchronous communication
- Store snapshots
  - Snapshot resolution may be lower than the main grid
  - Each snapshot requires own halo exchange
  - No actual I/O, so no collective communication

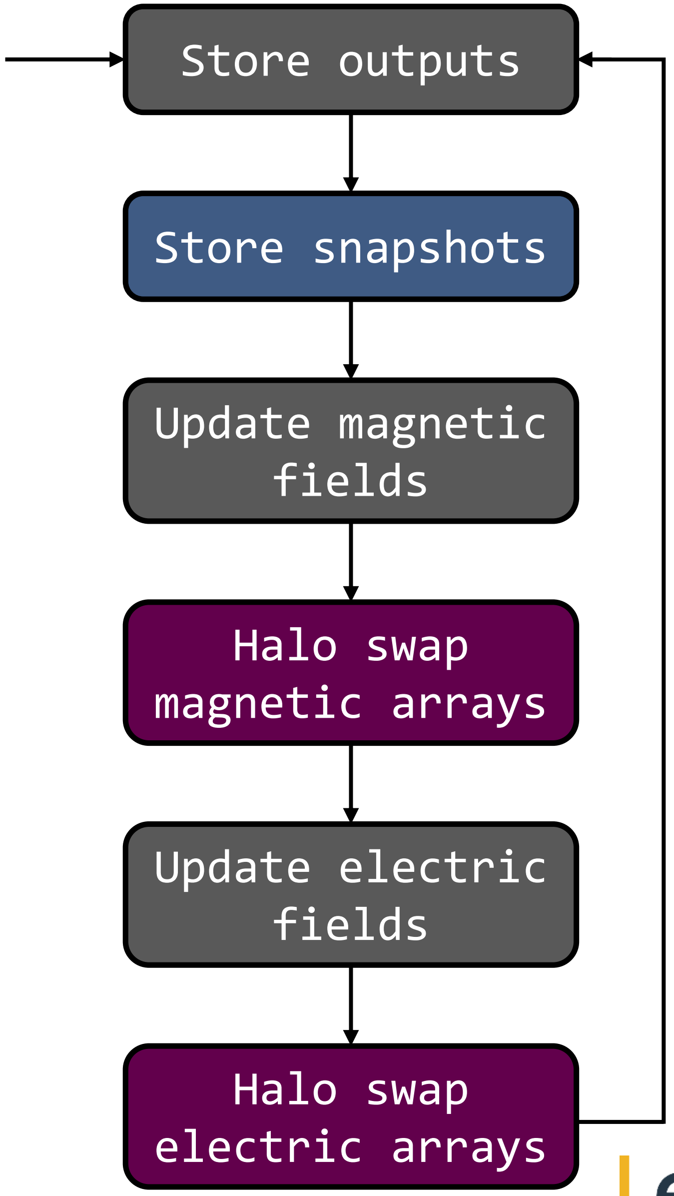

epcc

Model Building

- Ranks build their own local grid
- No OpenMP parallelisation for this part of the code
  - Lots of room for improvement with MPI
- Result is insensitive to the domain decomposition
- Ranks map from the global coordinate space to the local coordinate space
- Fractal objects and I/O objects were the biggest challenge

Single Node Performance

- Simulation uses ~ 53.2 GB of memory
- The node is fully populated throughout

```
1 MPI rank  → 128 OpenMP threads per rank
8 MPI ranks → 16  OpenMP threads per rank
Etc…
```

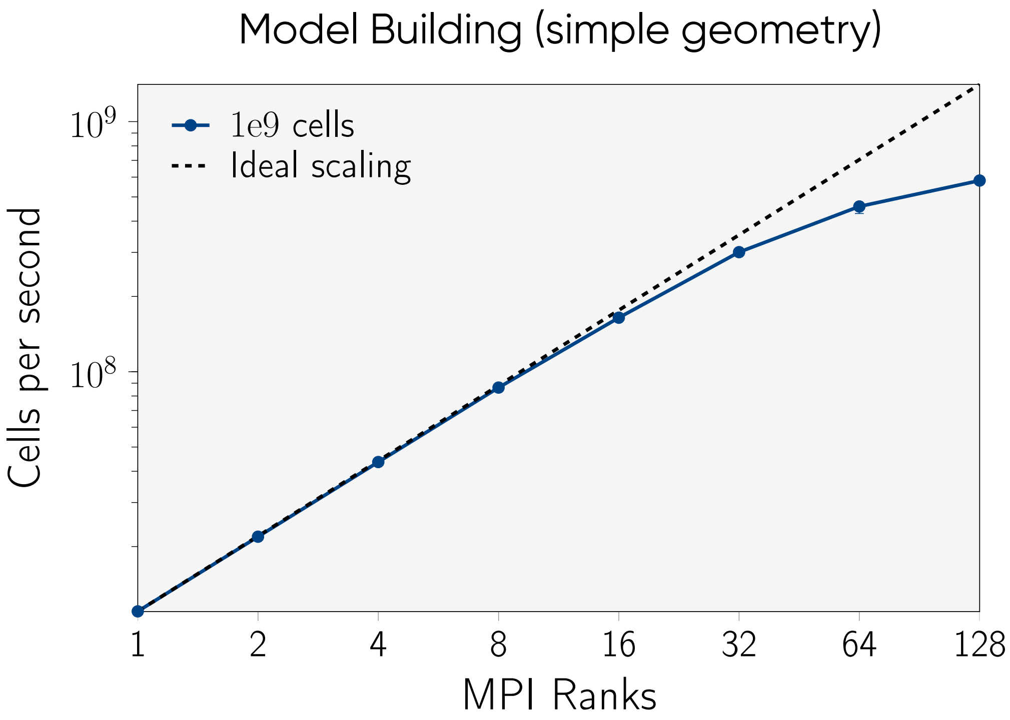

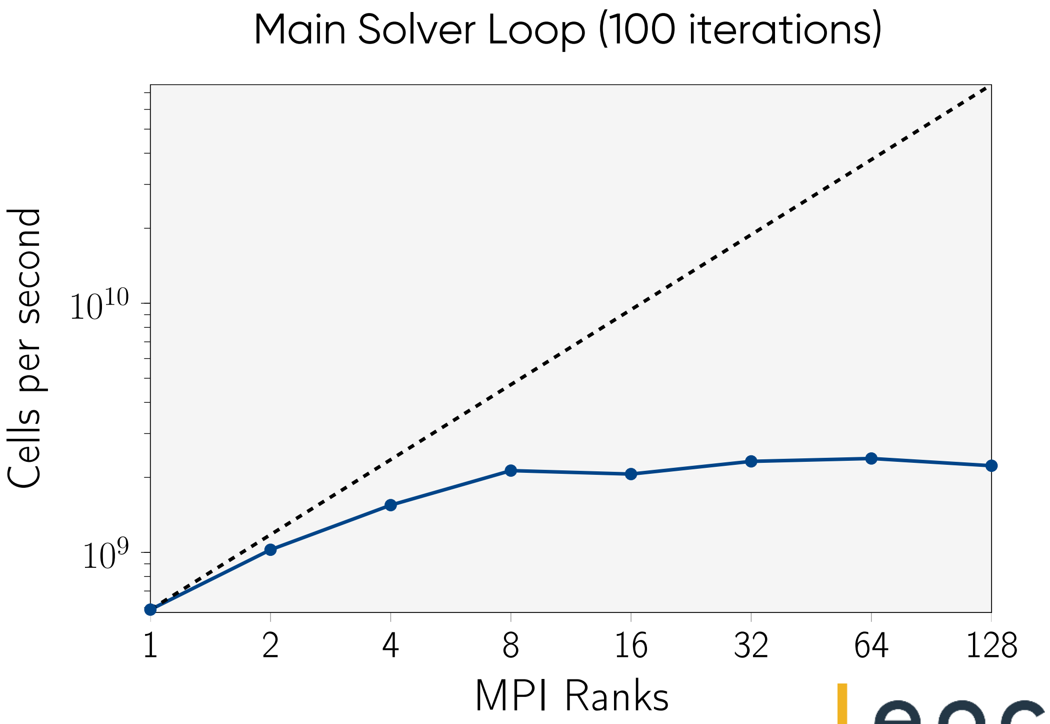

epcc

Multi Node Performance

- Chose the best performing single-node configuration:
  - 64 MPI ranks per node and 2 OpenMP threads per rank
- Largest model: 2.6×10^{11} cells, ~ 14.4 TB of memory across 64 nodes

Model Building (simple geometry)

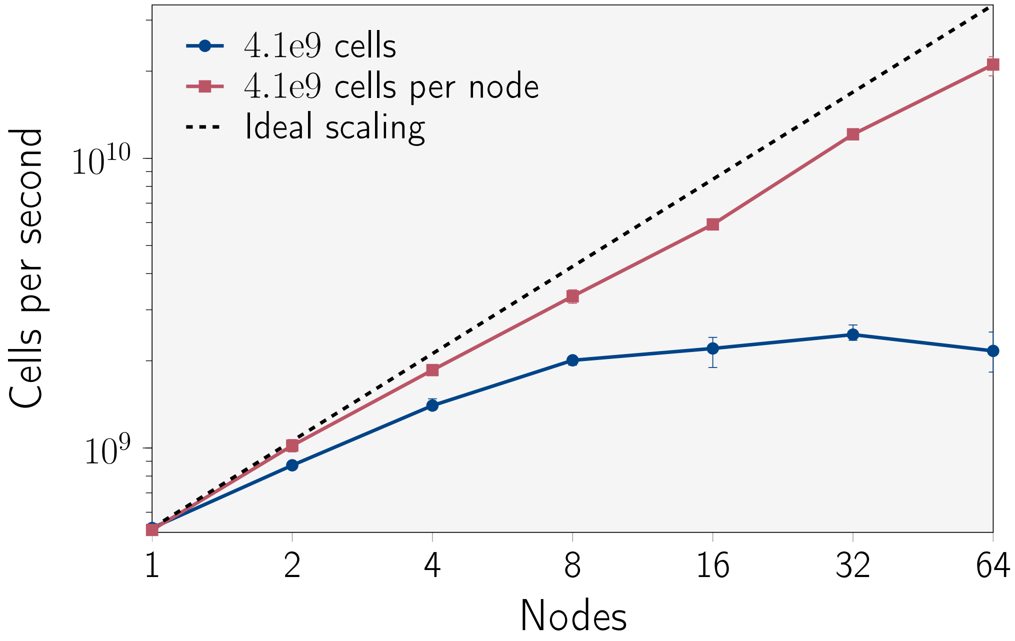

Main Solver Loop (100 iterations)

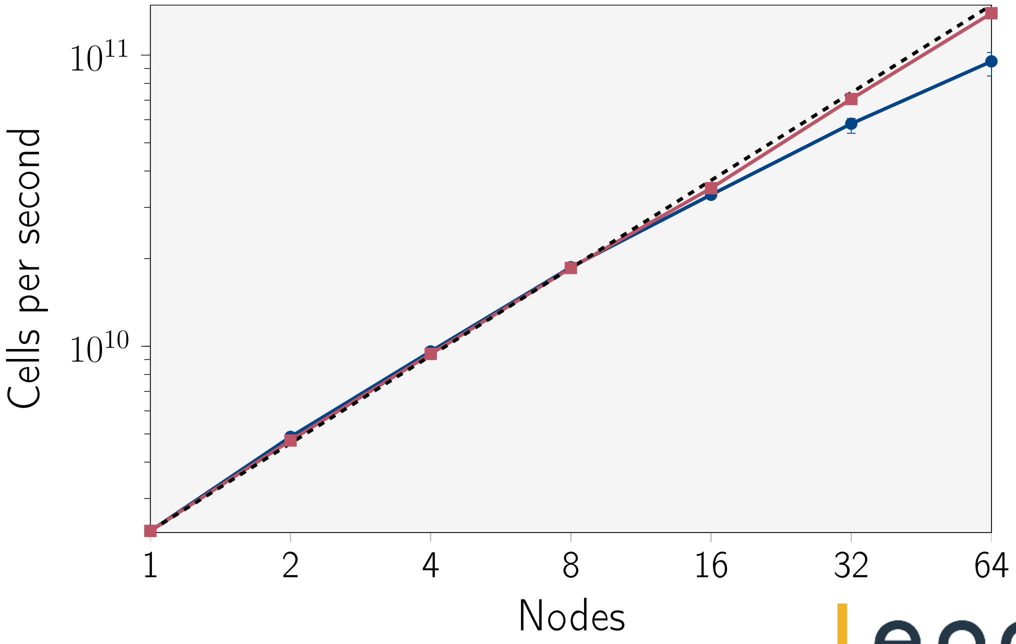

epcc

Model Building – Fractal Geometry

- Used for stochastic materials (e.g. soil models) and surface roughness
- Perform an FFT over a 2D or 3D array of random numbers
- Limits domain decomposition – must be 1 in at least one dimension
  - 1D (slab) or 2D (pencil) – not 3D
- Choice of decomposition can dramatically effect performance
- Needs to be reproducible in parallel

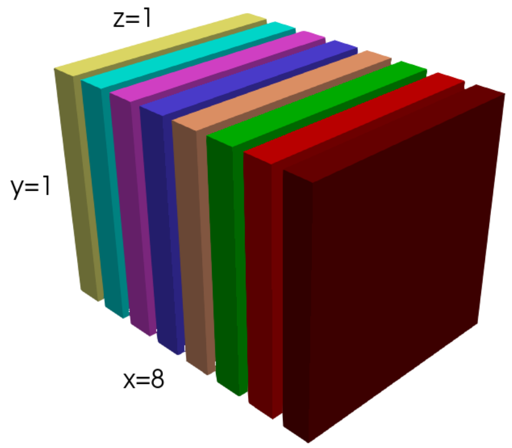

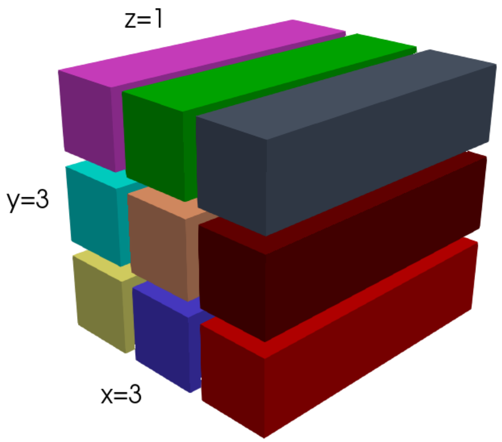

Model Building – Fractal Geometry

- Initial attempt ~100 times slower than serial baseline
  - Iterate over global grid and generate random numbers one at a time
  - Keep if within the local grid. Otherwise discard
- Instead calculate blocks of random numbers to either keep or discard

Implementation	MPI Ranks	OpenMP Threads	Time in `generate_fractal_volume()`	Percentage of total runtime in `generate_fractal_volume()`
Serial	-	32	34.4s	2.9%
Original MPI	8	16	3135.7s	82.7%
Updated MPI	8	16	24.2s	3.5%

Note: The MPI runs used `--mpi 1 2 4` as the decomposition. It is likely `--mpi 1 1 8` would improve the overall performance further.

VTKHDF for Parallel I/O

- HDF5 is well supported for HPC and Python
- VTKHDF gives advantages of HDF5 while directly supporting visualisation

- I/O performance effected by domain decomposition
- Currently support independent I/O
  - Likely to get better write performance with collective I/O

https://docs.vtk.org/en/latest/vtk_file_formats/vtkhdf_file_format/vtkhdf_specifications.html

Regression Testing with ReFrame

ReFrame

- Existing tests required manual inspection to check correctness
- Automated tests caught errors early
  - Full model regression tests – not unit tests
  - Can directly compare results from non-MPI tests with MPI tests
- Adding a new test requires:
  - A model input file
  - Typically 4-8 lines of code

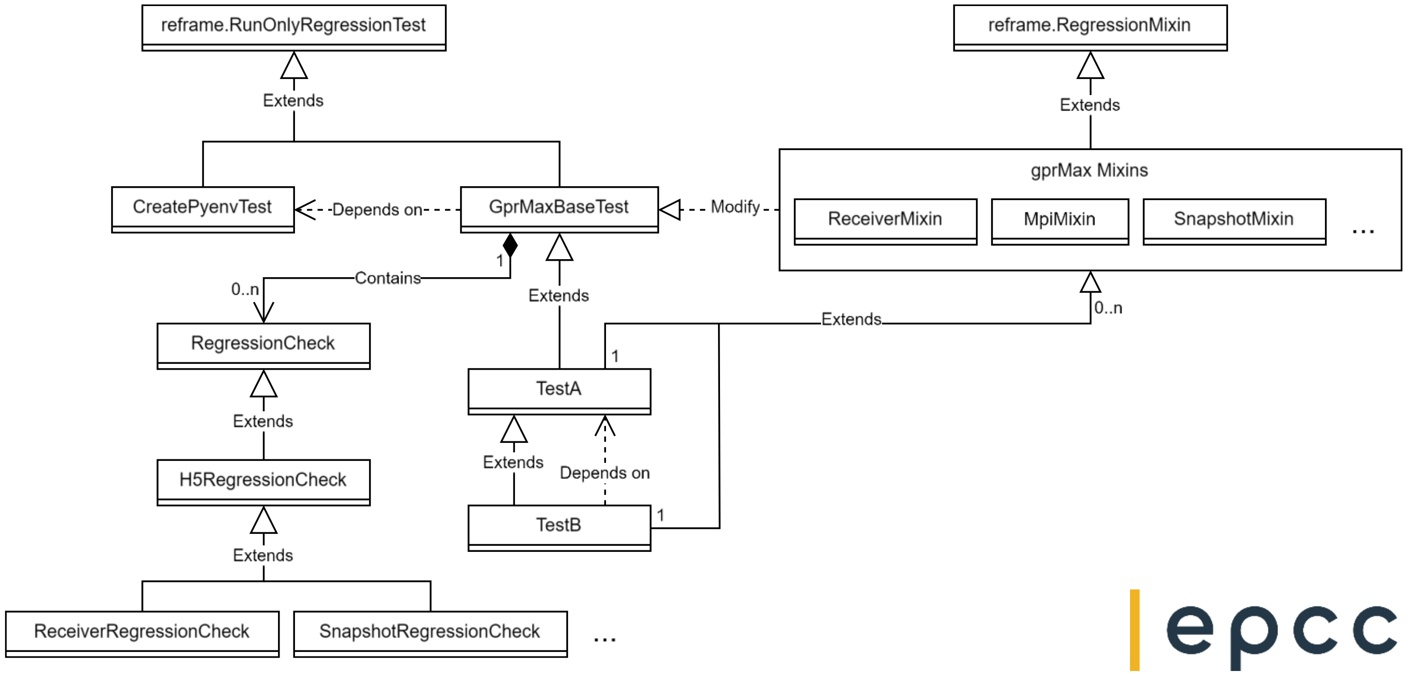

https://github.com/reframe-hpc/reframe

gprMax Visualisation – Sébastien Lemaire

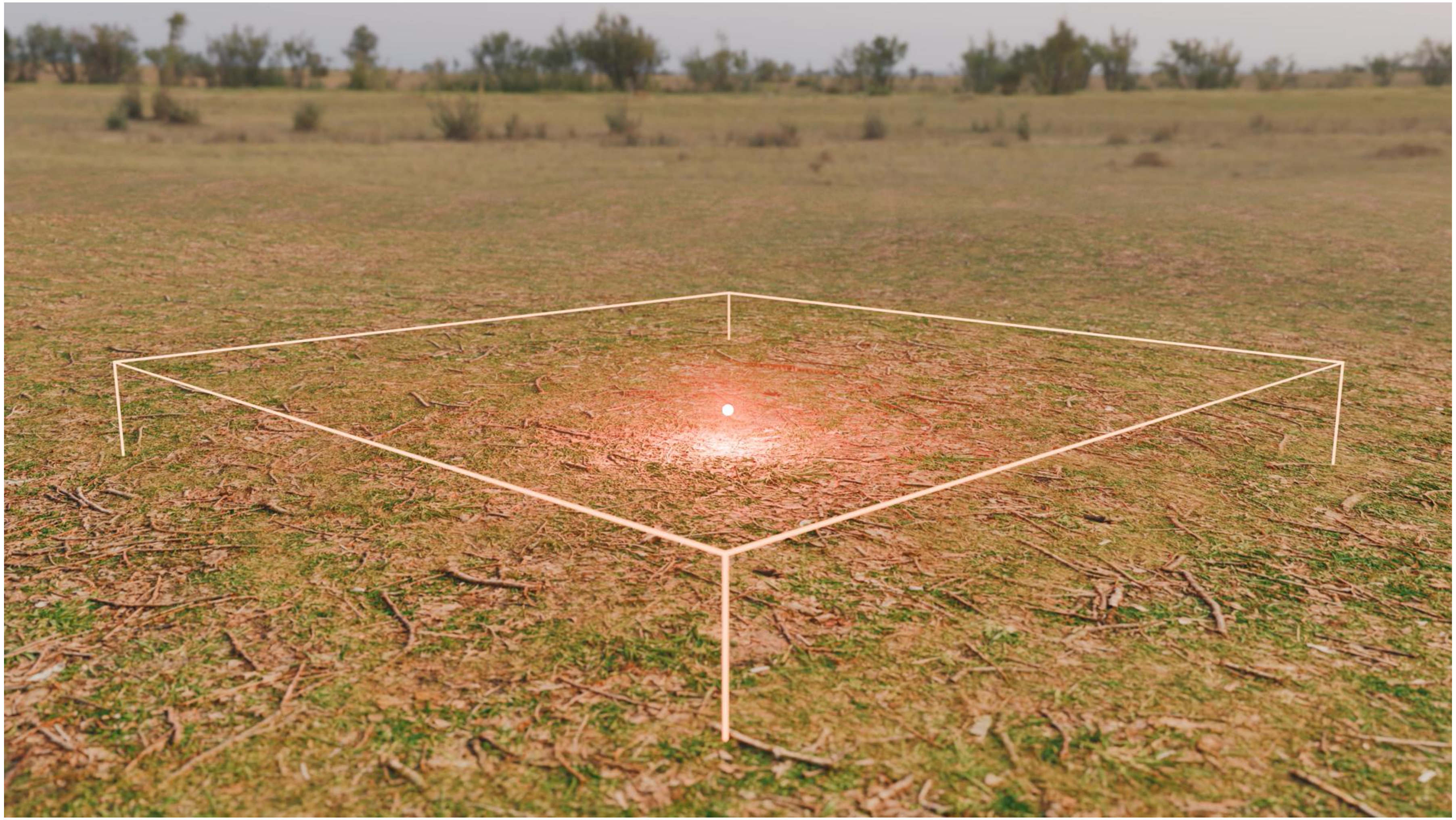

https://www.epcc.ed.ac.uk/research/scientific-visualisations

Project Team

- Craig Warren
- Antonis Giannopoulos
- James Richings
- Nathan Mannall

This work was funded under the embedded CSE programme of the ARCHER2 UK National Supercomputing Service (https://www.archer2.ac.uk).